ELSEVIER

Chemical Geology 161 (1999) 59–88

CHEMICAL GEOLOGY
INCLUDING
ISOTOPE GEOSCIENCE

www.elsevier.com/locate/chemgeo

$^{87}Sr/^{86}Sr$, $\delta^{13}C$ and $\delta^{18}O$ evolution of Phanerozoic seawater

Ján Veizer [a,b,*], Davin Ala [b,c], Karem Azmy [b], Peter Bruckschen [a], Dieter Buhl [a], Frank Bruhn [a,d], Giles A.F. Carden [a,e], Andreas Diener [a,f], Stefan Ebneth [a,g], Yves Godderis [b,h], Torsten Jasper [a], Christoph Korte [a], Frank Pawellek [a], Olaf G. Podlaha [a,i], Harald Strauss [a,j]

[a] *Institut für Geologie, Ruhr Universität, Bochum 44780, Germany*
[b] *Ottawa-Carleton Geoscience Centre, University of Ottawa, Ottawa, ON, Canada K1N 6N5*
[c] *17A Street SW, Calgary, AB, Canada T3T 4S4*
[d] *Leibniz-Labor für Altersbestimmung und Isotopenforschung, Christian-Albrechts Universität, 24158 Kiel, Germany*
[e] *Research and Development Service Offices, The University of Warrick, Coventry CV4 7AL, UK*
[f] *Fuhlrott Museum, Auer Schulstrasse 20, Wuppertal-Elberfeld 42103, Germany*
[g] *F.D. Züblin, Mathias-Brüggen Strasse 79, Cologne 50827, Germany*
[h] *Laboratoire de Physique Atmosphérique et Planétaire, Université de Liège, Liège 4000, Belgium*
[i] *Shell International Exploration and Production, PO Box 60, 2280 AB Rijswijk, Netherlands*
[j] *Geologisch-Paläoutologiselies Institut und Museum, Westphälische Wilhelms-Universität, 48149 Münster, Germany*

Received 11 December 1997; accepted 12 October 1998

Abstract

A total of 2128 calcitic and phosphatic shells, mainly brachiopods with some conodonts and belemnites, were measured for their $\delta^{18}O$, $\delta^{13}C$ and $^{87}Sr/^{86}Sr$ values. The dataset covers the Cambrian to Cretaceous time interval. Where possible, these samples were collected at high temporal resolution, up to 0.7 Ma (one biozone), from the stratotype sections of all continents but Antarctica and from many sedimentary basins. Paleogeographically, the samples are mostly from paleotropical domains. The scanning electron microscopy (SEM), petrography, cathodoluminescence and trace element results of the studied calcitic shells and the conodont alteration index (CAI) data of the phosphatic shells are consistent with an excellent preservation of the ultrastructure of the analyzed material. These datasets are complemented by extensive literature compilations of Phanerozoic low-Mg calcitic, aragonitic and phosphatic isotope data for analogous skeletons. The oxygen isotope signal exhibits a long-term increase of $\delta^{18}O$ from a mean value of about −8‰ (PDB) in the Cambrian to a present mean value of about 0‰ (PDB). Superimposed on the general trend are shorter-term oscillations with their apexes coincident with cold episodes and glaciations. The carbon isotope signal shows a similar climb during the Paleozoic, an inflexion in the Permian, followed by an abrupt drop and subsequent fluctuations around the modern value. The $^{87}Sr/^{86}Sr$ ratios differ from the earlier published curves in their greater detail and in less dispersion of the data. The means of the observed isotope signals for $^{87}Sr/^{86}Sr$, $\delta^{18}O$, $\delta^{13}C$ and the less complete $\delta^{34}S$ (sulfate) are strongly interrelated at any geologically reasonable (1 to 40 Ma) time resolution. All correlations are valid at the 95% level of confidence, with the most valid at the 99% level. Factor analysis indicates that the $^{87}Sr/^{86}Sr$, $\delta^{18}O$, $\delta^{13}C$ and $\delta^{34}S$ isotope systems are driven by three factors.

* Corresponding author. Department of Earth Sciences, Ottawa-Carleton Geoscience Centre, University of Ottawa, Ottawa, ON, Canada K1N 6N5. Tel.: +1-613-562-5800; fax: +1-613-562-5192; E-mail: veizer@geol.uottawa.ca

PII: S0009-2541(99)00081-9

The first factor links oxygen and strontium isotopic evolution, the second $^{87}Sr/^{86}Sr$ and $\delta^{34}S$, and the third one the $\delta^{13}C$ and $\delta^{34}S$. These three factors explain up to 79% of the total variance. We tentatively identify the first two factors as tectonic, and the third one as a (biologically mediated) redox linkage of the sulfur and carbon cycles. On geological timescales (≥ 1 Ma), we are therefore dealing with a unified exogenic (litho-, hydro-, atmo-, biosphere) system driven by tectonics via its control of (bio)geochemical cycles.

Keywords: Seawater; Phanerozoic; Isotopes; Strontium; Oxygen; Carbon

1. Introduction

The *Sr isotopic composition of past seawater*, as monitored by marine carbonate shells and rocks, can be utilized as a proxy parameter for tectonic evolution of the Earth System, because the $^{87}Sr/^{86}Sr$ variations reflect principally the waxing and waning of Sr input from rivers ('continental' flux) vs. the input from the submarine hydrothermal systems ('mantle' flux) (Faure, 1986; Taylor and Lasaga, this issue). The general trends of $^{87}Sr/^{86}Sr$ variations for Phanerozoic seawater have been sketched already in the pioneering studies of Peterman et al. (1970), Veizer and Compston (1974) and Burke et al. (1982). The published 'curve' of the last authors served subsequently as a baseline for all follow-up studies. The last decade, however, witnessed a considerable advance in instrumental precision, sample preparation and in better geological constraints, particularly in stratigraphic assignment of samples. This resulted in a considerably tighter delineation of the secular marine isotope trend and opened the stage for utilization of Sr isotopes as a correlation and dating tool, 'isotope stratigraphy'. This stage of research has been summarized in DePaolo and Ingram (1985), Elderfield (1986), Veizer (1989), McArthur (1994) and Smalley et al. (1994). Nevertheless, the utility of this new tool has been restricted mostly to the Cenozoic, because of the steep and well-defined rise in marine $^{87}Sr/^{86}Sr$ ratio. Apart from the steep slope, the major reason for delineation of such a well-defined trend has been the fact that this young portion of the geologic record has a relatively well-resolved and detailed stratigraphy and that sediments of this age contain shells that were only marginally affected by the vicissitudes of diagenesis.

In theory, it should be possible to define similar well-constrained trends also for other Phanerozoic intervals with equally steep slopes and thus extend the utility of the 'isotope stratigraphy' into the Mesozoic and Paleozoic (Veizer et al., 1997a). The constraining factors in achieving this goal are not so much the instrumental capabilities, because for many laboratories intra- and interlaboratory reproducibility routinely falls within $\pm 25 \times 10^{-6}$ limits (Thirwall, 1991; McArthur, 1994), but the preservation and resolution of the geologic record.

The $\delta^{13}C$ *of ancient oceans* (e.g., Clayton and Degens, 1959; Schidlowski et al., 1975; Veizer and Hoefs, 1976) was for a long time regarded as essentially invariant, but with a considerable noise, around 0‰ PDB. Only in the 1980s was it realized that this noise contains a real oscillating secular signal (Scholle and Arthur, 1980; Veizer et al., 1980; Arthur et al., 1985; Shackleton, 1985). In contrast to the below-discussed oxygen isotopes, the primary nature of the $\delta^{13}C_{carbonate}$ secular trend has not been seriously challenged. The reason is that diagenetic recrystallization of carbonates is accomplished in a system with a low water/rock ratio for carbon, and a high ratio for oxygen (Banner and Hanson, 1990; Banner, 1995; Jacobsen and Kaufman, this issue). Diagenetic stabilization of carbonates therefore results in transposition of carbon from a precursor to a successor mineral phase.

The above oscillations in the $\delta^{13}C_{carbonate}$ trend are being increasingly utilized for correlation and isotope stratigraphy (e.g., Knoll et al., 1986; Derry et al., 1992). This tool, however, is subject to additional limitations if compared to Sr isotopes. The major difference arises from the fact that $\delta^{13}C_{carbonate}$ at any given time shows a considerable spread of values due to spatial variability of oceanic $\delta^{13}C_{\Sigma CO_2}$ (e.g., Kroopnick, 1985) and due to biological factors of shell formation (McConnaughey and Whelan, 1997). The complications arise not so much during

logging of a single well or a profile, but can become considerable if unrelated sequences or wells are compared. Nonetheless, large peaks can serve as correlation markers, particularly in the Precambrian (Kaufman et al., 1992). In addition, the secular $\delta^{13}C_{carbonate}$ trend is increasingly utilized as a proxy for determining oceanic paleoproductivity/preservation patterns, ancient pCO_2 and pO_2 states, and similar paleoenvironmental phenomena (Berner et al., 1983; Berner, 1994; Kump and Arthur, this issue).

The $^{18}O/^{16}O$ *composition of ancient oceans* is one of the perennial and most controversial issues of isotope geochemistry. Commencing with the nascent stages of isotope geochemistry, it has been realized (Baertschi, 1957; Clayton and Degens, 1959) that oxygen isotopic composition of carbonates becomes progressively more depleted in ^{18}O with increasing age of the rocks. This trend for carbonates (and other chemical marine sediments) has been confirmed by many studies (e.g., Veizer and Hoefs, 1976) and its validity is not disputed. It is the implications of such observations that result in a sharp division within the scientific community. If essentially a primary feature, the implications could be one or all of the following: (1) seawater $\delta^{18}O$ must have changed in the course of the Phanerozoic (e.g., Weber, 1965; Perry and Tan, 1972; Hudson and Anderson, 1989); (2) the early oceans must have been much warmer than today, up to $\sim 70°C$ (Knauth and Epstein, 1976; Kolodny and Epstein, 1976; Karhu and Epstein, 1986); or (3) they were stratified, with deep waters being generated by sinking of salty brines from extensive evaporation at low latitudes (Brass et al., 1982; Railsback, 1990). Objections to alternative (1) arise from studies of the oceanic crust and its ancient counterparts (Gregory and Taylor, 1981) and from model considerations (Muehlenbachs and Clayton, 1976; Gregory, 1991; Muehlenbachs, 1998), both claiming that the $\delta^{18}O$ of ocean water is, and has been, buffered at $\sim 0‰$ SMOW by rock/water interactions in hydrothermal cells at oceanic ridges. For alternative (2), the persistence of essentially the same faunal assemblages and the recurrence of ice ages throughout the Phanerozoic are difficult to reconcile with the advocated warm temperatures (Veizer et al., 1986). Finally, for alternative (3), the implied permanent saline stratification would be difficult to sustain and, even if sustainable, it could account for no more than $\sim 1.5‰$ ^{18}O depletion in the near-surface oceanic layer (Railsback, 1990).

The above considerations, and the observation that advancing diagenetic recrystallization of carbonate (and other) phases results in ^{18}O depletion, either due to involvement of meteoric waters or to elevated temperatures, led one group of researchers to argue that the $\delta^{18}O$ secular trend is essentially a diagenetic feature (Degens and Epstein, 1962; Killingley, 1983; Land, 1995). Resolution of this secondary vs. primary dilemma is of utmost importance, because the $\delta^{18}O$ could potentially serve as a powerful paleoceanographic tracer for the entire Phanerozoic.

In this contribution, due to space restrictions, we concentrate solely on documentation of the trends in order to make the datasets available to the scientific community. Their interpretations and implications for the $\delta^{13}C$ are discussed by other authors in this volume (Hayes et al., this issue; Kump and Arthur, this issue). For the $\delta^{18}O$, the resolution of the primary vs. secondary nature of the Phanerozoic trend is a precondition for any argumentation dealing with consequences. We shall therefore concentrate on this issue only, leaving the model implications for future consideration.

Because of the potential utility of $^{87}Sr/^{86}Sr$, $\delta^{13}C$ and $\delta^{18}O$ secular trends for resolution of paleoceanographic, paleoecological and stratigraphic questions, it is essential to define these trends as tightly as possible. Here, we introduce a new set of paleoseawater curves for the Phanerozoic. In order to minimize the impact of diagenetic resetting of the signal, we have concentrated on material that is relatively resistant to diagenetic alteration. Similarly, in order to attain high resolution, we resampled 'complete' and well-dated sequences. Nevertheless, fulfillment of these two requirements, in particular the temporal assignment of samples, is a complex task that requires some introductory discussion.

2. Completeness of the sedimentary record and isotopic ages

Any given stratigraphic section only intermittently records the passage of geological time (Dingus, 1984). On a global scale, the volume of sedimentary

rocks decreases with age because the record becomes progressively less complete with time. Within any sedimentary sequence, there are hiatuses which represent periods of non-deposition, erosion and/or diagenesis. Stratigraphic sections spanning greater temporal intervals have a greater opportunity of incorporating more hiatuses and hiatuses spanning longer periods of time (Sadler, 1981; Korvin, 1992). Determining the stratigraphic position and duration of a hiatus within a section is often problematic. The end result is a progressive decrease in the completeness of the stratigraphic record with increasing age.

In general, sequences often have erosional or non-depositional contacts which are difficult to identify from lithological parameters alone. In these situations, biostratigraphy, absolute dating and magnetostratigraphy are often utilized. Unfortunately, each method has its limitations. Presently, the highest resolution can be achieved with biostratigraphy, with a resolution limit rarely better than 0.5 Ma and more often on the order of 1 Ma or more. As a result, the upper limit for using this method for hiatus identification cannot be better than 0.5 Ma. In addition, bioturbation can effectively homogenize sediments in the upper 10–15 cm, rendering any stratigraphic method meaningless at scales less than 15 cm (Anders et al., 1987). If sediment accumulation is slow, then the effect of bioturbation on the resolution may become geologically significant.

Stratigraphers define a complete section as one which has no gaps larger than each time unit of a specific scale (Anders et al., 1987). As the resolution improves (corresponding to shorter time scales), there is a corresponding decrease in the perceived completeness of the section. Therefore, improved sampling accuracy will result in an overall decrease in the perceived completeness of the stratigraphic section (Schindel, 1982; Dingus, 1984). On average, it is estimated that only 1/30th of the elapsed time is represented by sediments (Algeo and Wilkinson, 1988; Miall, 1994).

The above constraints are compounded by problems with assignment of 'absolute', or more correctly 'isotopic', ages to particular samples. In order to enable comparison with other datasets, we consistently utilized the time scale of Harland et al. (1990), despite the fact that many of these 'ages', including the commencement of the Phanerozoic at 570 Ma ago (rather than 543 Ma; Bowring and Erwin, 1998), are today not accepted anymore. The uncertainties in 'age' estimates for epochs and stages are usually several million years, larger than the entire duration of many stages. For example, the estimated duration of the Eifelian of ~ 4 Ma is bracketed by isotopic ages of 386 ± 5 to $382 + 9/-14$ Ma (Harland et al., 1990). This interval encompasses some five conodont biozones, each arbitrarily assigned an isotopic age by linear extrapolation between these two estimates that have large experimental errors.

Because of the above complications, we have concentrated on sedimentary sequences that were as complete as possible, preferably stratotypes, providing they contained suitable material (shells) for isotopic studies. The correlation of samples from different localities was based on biostratigraphy (biozones) and not on 'isotopic ages'. The relative 'age' within the same sequence and biozone was based on stratigraphic superposition. Unfortunately, when comparing distant Paleozoic and Mesozoic sequences, the best that we could accomplish was a correlation to a biozone resolution. This will be important when discussing higher level oscillations in the isotope signal.

3. Sample selection

In order to constrain as much as possible post-depositional alteration of the isotope signal, we have concentrated on samples that are relatively resistant to diagenesis. The preferred material is the low-Mg calcite of marine skeletons, such as brachiopods, belemnites and foraminifera. Keeping in mind that the Cenozoic portion of the isotope record has been extensively studied, chiefly due to DSDP, we have concentrated on the Paleozoic and Mesozoic. These left brachiopods and belemnites as the only abundant and stratigraphically widespread fossils with low-Mg calcitic skeletons. Furthermore, for brachiopods, we have utilized only the so called 'secondary' (i.e., interior) layer, because its elongated calcitic fibers showed the highest degree of preservation, up to sub-micron levels. The details of our approach and examples of the exceptional degree of preservation of many shells have been documented in Diener et

al. (1996), Veizer et al. (1997a,b), Azmy et al. (1998) and Bruckschen et al. (1999). For the Mesozoic belemnites, the approach has been similar, except that the samples were drilled within a single 'lamina' of the rostrum, parallel to its elongation (Podlaha et al., 1998).

For Sr isotopes, in the initial stages, we have concentrated also on conodonts, believing that because of their superior stratigraphic resolution and the high Sr content of their phosphatic skeletons, they may yield a $^{87}Sr/^{86}Sr$ curve for the Phanerozoic seawater with the highest temporal resolution attainable. Comparison with brachiopod data showed, however, that conodonts, even at a conodont alteration index (CAI) as low as 1.5, had $^{87}Sr/^{86}Sr$ ratios that were at best comparable to coeval brachiopods, but mostly the measurements were more radiogenic (Ebneth et al., 1997; Veizer et al., 1997a). These, and the textural and proton-induced X-ray emission (PIXE) trace element studies (Bruhn et al., 1997), showed that conodonts exchanged about 1/3 of their Sr with the surrounding rock matrix. In suitable matrix, such as pure carbonates, conodonts may still retain their near-original $^{87}Sr/^{86}Sr$ values, but mostly the values are $\sim 5 \times 10^{-5}$ more radiogenic (Ebneth et al., 1997). Because of these reasons, we have discontinued conodont studies, except for the time intervals where the low-Mg calcitic fossils were rare or absent, such as the Cambrian and the early Triassic.

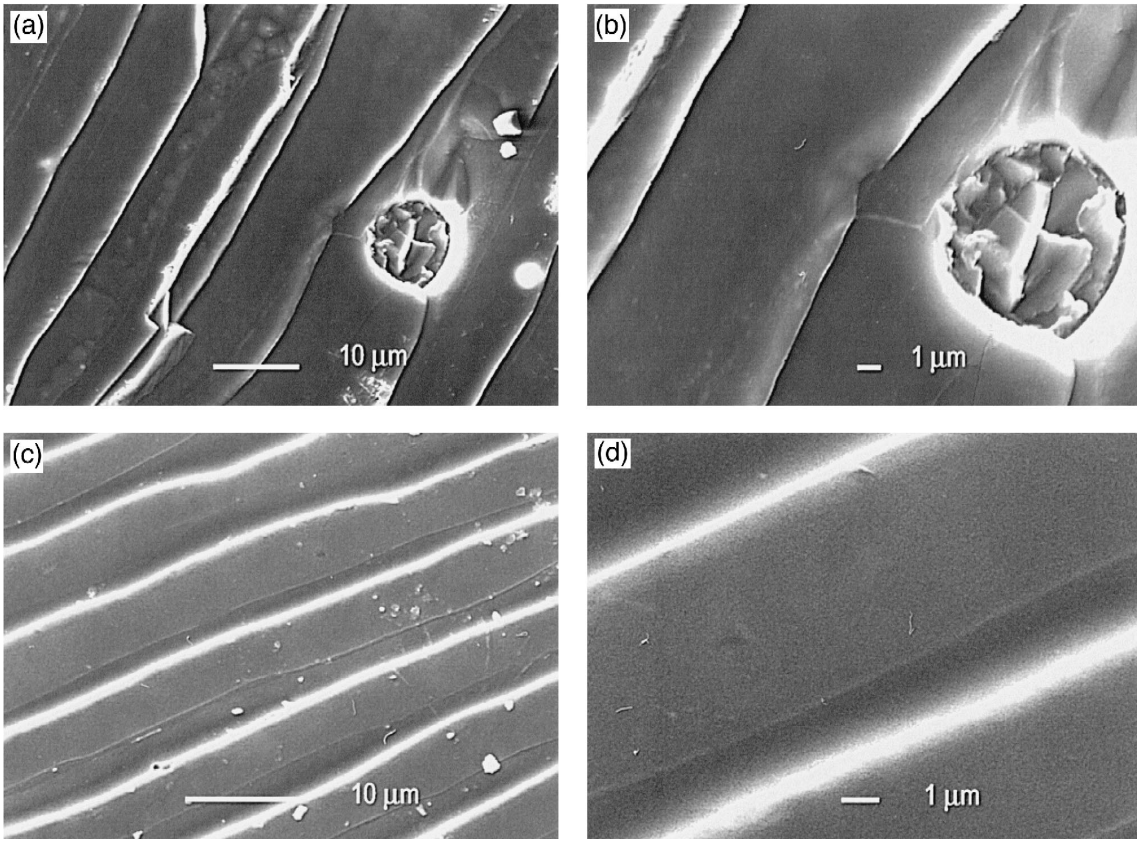

Fig. 1. The SEM photos of representative brachiopods. Note the excellent preservation of the secondary shell layer (from Azmy, 1996). (a) *Isorthis amplificata* (B27; Wenlock, Much Wenlock, UK) shell, with punctae filled by secondary calcite. The punctae calcite has intensive yellowish cathodoluminescence, as opposed to no or only intrinsic blue luminescence of the shell. The isotopic and chemical characteristics of the shell are the following: $\delta^{18}O = -5.50‰$, $\delta^{13}C = +0.39‰$, Mn = 307 ppm, Sr = 1934 ppm. (b) As (3a) at higher magnification. (c) *Delthyris elevata* (EK 38-7; Pridoli, Ohesaare Cliff, Estonia): $\delta^{18}O = -5.50‰$, $\delta^{13}C = -0.50‰$, Mn = 104 ppm, Sr = 1328 ppm. (d) As (3c) at higher magnification.

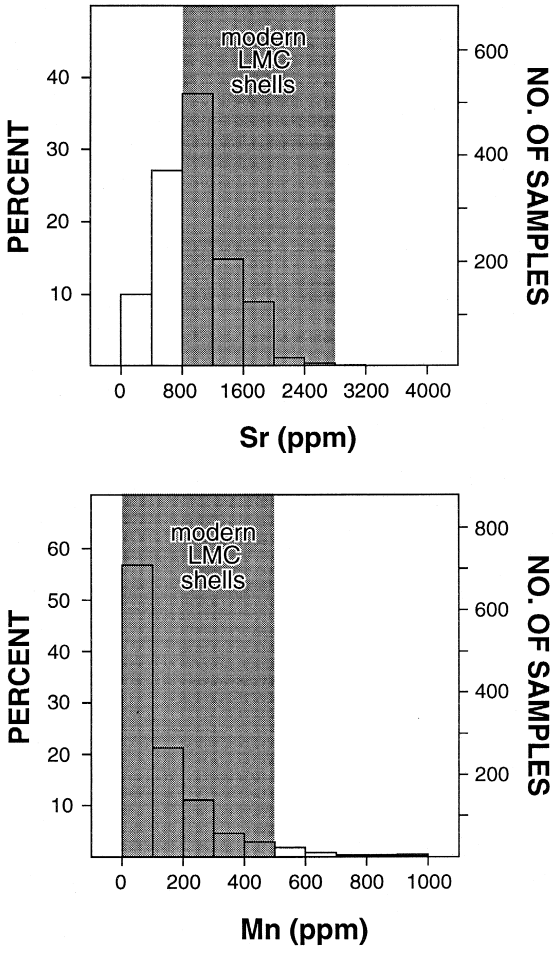

Fig. 2. Histograms of Sr ($n = 1370$) and Mn ($n = 1267$) concentrations in the studied brachiopods and belemnites.

The samples were screened for their degree of preservation by optical (transmitted light, cathodoluminescence and scanning electron microscopy, SEM) techniques. These have been documented in Bruhn et al. (1995) and Bruckschen et al. (1995a,b). Fig. 1 demonstrates an example of excellent preservation of textures on sub-micron scale. This optical screening was complemented by trace element evaluation by wet chemical techniques (inductively coupled plasma atomic emission spectroscopy [ICP-AES], atomic absorption spectroscopy [AAS]) on aliquots remaining after phosphoric acid liberation of CO_2 for stable isotope measurements (Coleman et al., 1989) and by PIXE spot analyses on thin sections. Based on the wet chemical approach, some 2/3 of all studied samples have Sr and Mn concentrations comparable to modern low-Mg calcitic shells (Fig. 2). The remaining 1/3, mostly with Sr content < 800 ppm, may or may not have suffered some diagenetic loss of Sr, since concentrations as low as 200 ppm have been reported for modern brachiopods (Morrison and Brand, 1986; Brand, 1989b). Note also that recrystallization, unless at exceptionally high water/rock ratios, does not necessarily result in resetting of $^{87}Sr/^{86}Sr$ or $\delta^{13}C$ values. For carbon, this is because of the earlier-discussed low water/rock ratios of the respective diagenetic systems. For strontium, due to the fact that D_{Sr} (calcite) is < 1, recrystallization happens in a partially open system buffered by the dissolving carbonate phase (Veizer, 1983). Alternatively, the lower Sr concentrations may be, in part, due to inclusion of distinct small domains of secondary calcites, and not to partial recrystallization, leaving the bulk of the shell unaltered. The presence of such secondary calcites can usually be detected by optical means (Fig. 3), particularly cathodoluminescence, and these calcites have also distinctive chemical (Table 1) and isotopic signatures (Bruckschen et al., 1995a; Bruhn et al., 1995).

4. Samples

The present study is based on several thousand samples of Cambrian to Cretaceous ages. These were collected in Canada (Anticosti Island, Ontario), USA (Utah, Oklahoma, Texas, Ohio, Kentucky, Missouri, New York), Ireland, England, Wales, Spain, Italy, Belgium, Germany, Poland, Norway (including

Fig. 3. (Top) Cathodoluminescence photomicrograph of a Carboniferous punctate brachiopod (sample PB 192a). Note the bright yellow luminescence of the punctae that are filled by diagenetic calcite. (Bottom) PIXE elemental map of the dark square in the top figure. Step size 10 μm. Note that the punctae are typified by Sr depletions (light domains) and simultaneous Mn enrichments (dark domains). The trace element data are in Table 1. Punctate brachiopods, except for demonstration purposes, were avoided in the present study. Modified from Bruhn (1995) and Bruckschen et al. (1995a).

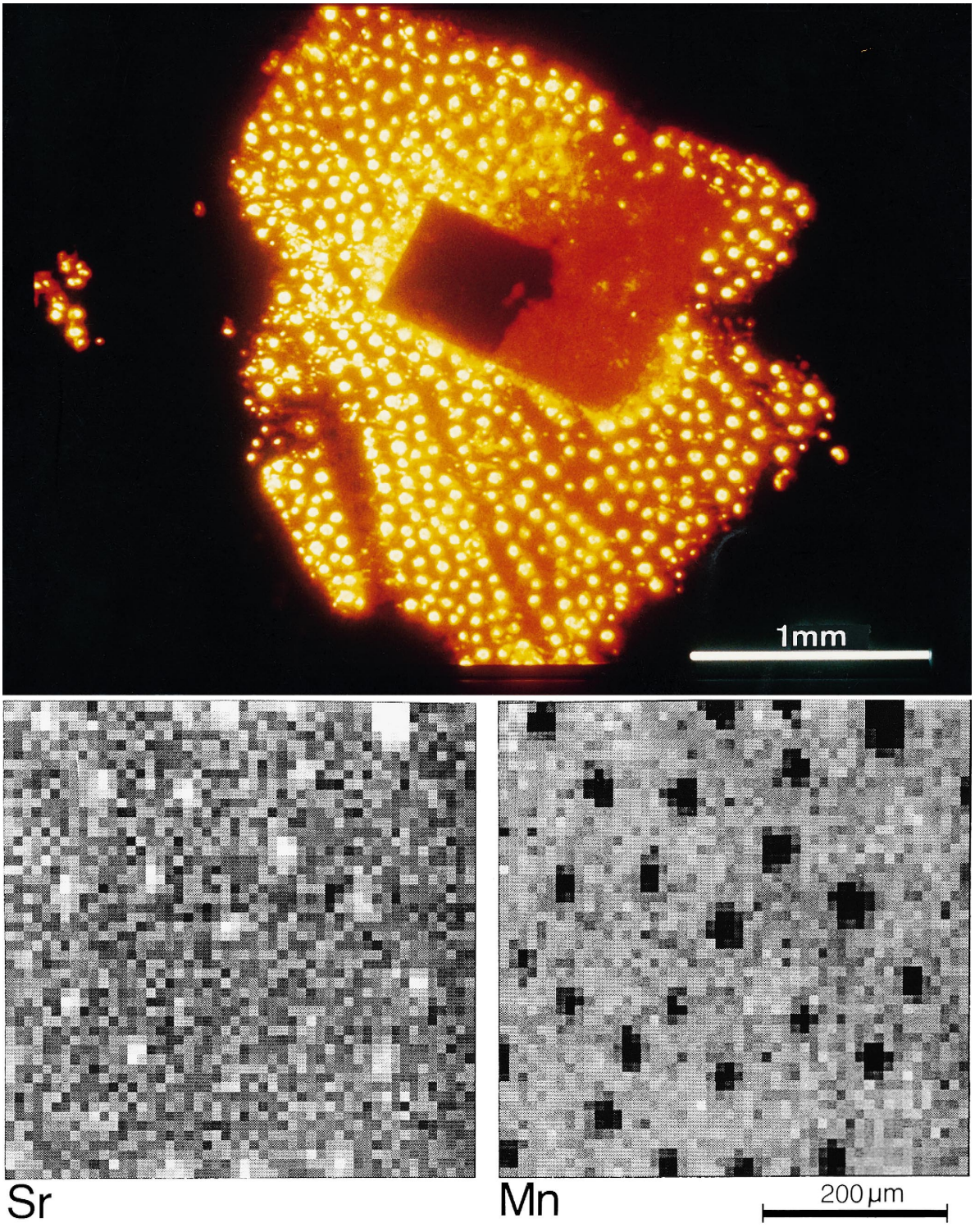
1mm
Sr
Mn
200 µm

Table 1
The PIXE trace element concentrations for a Carboniferous punctate brachiopod (sample PB 192a)

	Mn		Fe		Sr	
	Shell	Punctae	Shell	Punctae	Shell	Punctae
	33	1810	40	733	1042	518
	20	3699	35	9261	977	217
	27	2043	36	722	969	379
	36	5040	73	1069	953	223
Mean	29	3148	48	2946	985	334
σ	8	1501	22	4833	12	92

Svarlbad), Sweden (including Gotland), Estonia, Latvia, Lithuania, Ukraine (Donetsk basin, Podolia), Austria, Slovakia, Hungary, Russia (Moscow basin, St. Petersburg area, Urals, western Siberia), Mo-

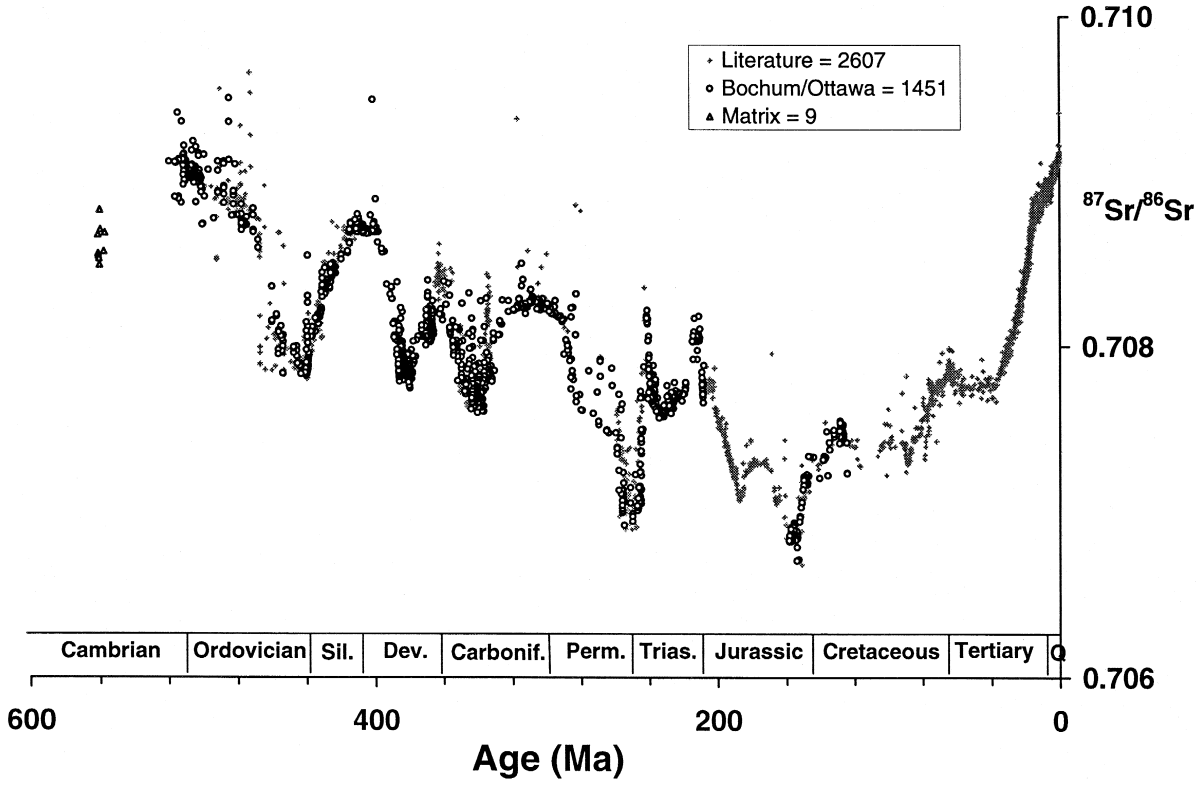

Fig. 4. $^{87}Sr/^{86}Sr$ variations for the Phanerozoic based on 4055 samples of brachiopods ('secondary' layer only for the new Bochum/Ottawa measurements), belemnites and conodonts, and nine samples of micritic matrix. Normalized to NBS 987 of 0.710240. The literature data (foraminifera, belemnites and conodonts) are from the following sources: Peterman et al. (1970), Dash and Biscaye (1971), Veizer and Compston (1974), Brass (1976), DePaolo and Ingram (1985), Koepnick et al. (1985), Hess et al. (1986, 1989), Popp et al. (1986c), McKenzie et al. (1988, 1993), Hodell et al. (1989, 1990, 1991), Brand (1991), Martin and McDougall (1991, 1995), Bertram et al. (1992), Dia et al. (1992), Barrera et al. (1993), Kürschner et al. (1993), Whittaker and Kyser (1993), Banner and Kaufman (1994), Cummins and Elderfield (1994), Denison et al. (1994), Hodell and Woodruff (1994), McArthur et al. (1994), Oslick et al. (1994), Quinn et al. (1994), Jones et al. (1994a,b), Chaisi and Schmitz (1995), Farrell et al. (1995), Ruppel et al. (1996), Wenzel (1997), Qing et al. (1998).

rocco, south China, Australia (Queensland, Northern Territory) and New Zealand. They have been collected (assembled) and described by the following researchers and publications: Cambrian (S. Ebneth), Ordovician (G.A.F. Carden), Silurian (Azmy, 1996; Azmy et al., 1998, 1999), Devonian (Diener, 1991; Ebneth, 1991; Pawellek, 1991; Fauville, 1995; Golks, 1995; Ala, 1996; Diener et al., 1996; Ebneth et al., 1997), Carboniferous (Bruckschen et al., 1995b, 1999; Bruckschen and Veizer, 1997), Permian (Jasper, 1999), Triassic (Korte, 1999) and Jurassic/Cretaceous (Podlaha, 1995; Podlaha et al., 1998, Podlaha et al., this issue). Judging from paleogeographic reconstructions of Scotese et al. (1994), most of these samples originate from tropical regions (30°N to 30°S) of the paleoceans, with few from higher paleolatitudes. From this collection, some 1500 samples of brachiopods and belemnites (and additional conodonts) have been selected for further Sr, O and C isotope studies and the details of their descriptions, including chemistry, isotopes, geology and location, are available in the above publications or in the summary tables posted on the Web site: http://www-ep.es.llnl.gov/germ/evolution.html or http://www.science.uottawa.ca/geology/isotope_data/.

5. Phanerozoic $^{87}Sr/^{86}Sr$ trend

The summary of Sr isotope data for Phanerozoic seawater (Fig. 4) is based solely on measurements on fossils. The Cenozoic and late Cretaceous part is from the literature and based chiefly on foraminifera. The remaining literature data, and all of Bochum/Ottawa measurements, are based on brachiopods, belemnites and conodonts. The sole exceptions are the matrix (micrite) samples for the early Cambrian that were incorporated because of the lack of suitable fossils. The 'curve' resembles the one by Burke et al. (1982), but it differs in detail and is more tightly constrained. Where larger spread of data exists, such as the radiogenic mid-Permian Chinese samples (Jasper, 1999), it is dealt with in the publication describing these particular periods. However, the

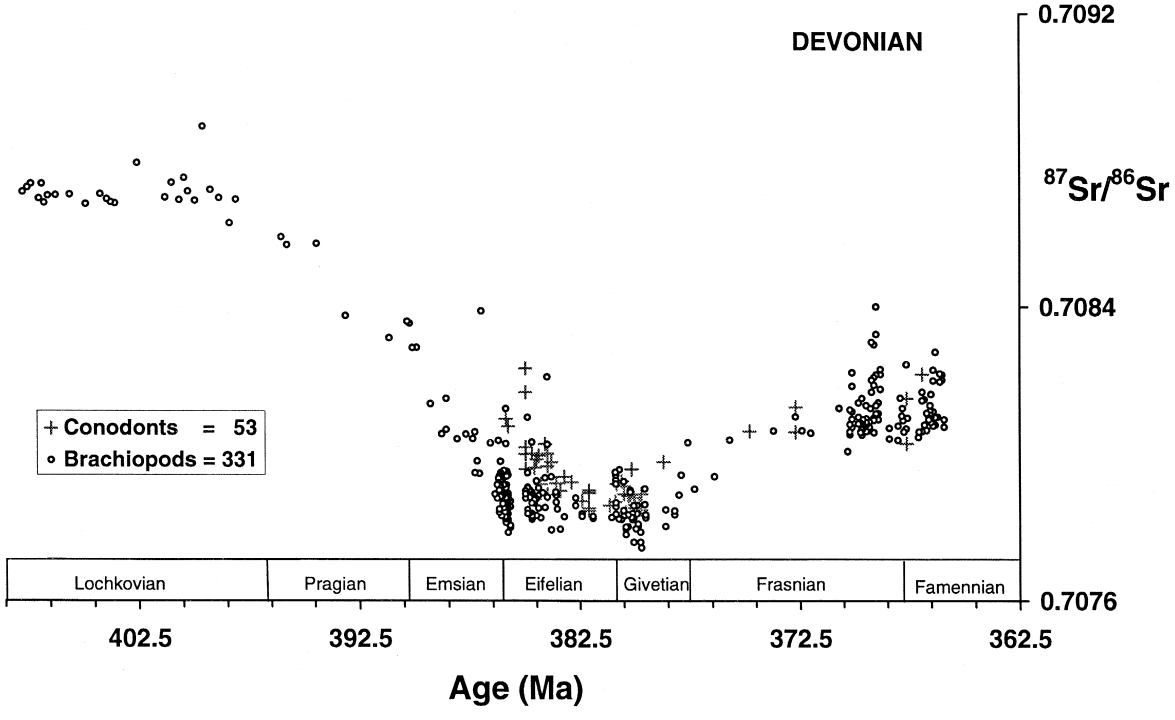

Fig. 5. $^{87}Sr/^{86}Sr$ variations during the Devonian (new Bochum/Ottawa data only).

clumping of data (cf. Devonian and Carboniferous) is mostly a reflection of a large number of measurements, with higher-order oscillations compressed along the temporal axis (cf. Bruckschen et al., 1995b, 1999; Bruckschen and Veizer, 1997).

Taking the Devonian as an example (Fig. 5), the higher-order oscillations, based on 384 samples, are well-illustrated. The secular trend shows a continuous decline through the Lower Devonian, a plateau in the Middle Devonian, a rise through the Frasnian and another plateau in the Upper Frasnian and Famenian. This figure also illustrates that conodonts are usually somewhat more radiogenic than coeval brachiopods. Furthermore, even at this resolution, some clumping still persists, such as at the Emsian/Eifelian and Frasnian/Famenian transitions. Again, the major culprit is the presence of still higher-order fluctuations in a compressed time scale. For the Middle Devonian, this was illustrated in Diener et al. (1996) (their Fig. 6), where it was also pointed out that the geological reproducibility of the Sr isotope pattern in profiles only several kilometers apart was no better than 5×10^{-5}. Thus, only the oscillations in excess of this range could be resolvable on regional to global scales.

Another constraining issue is the problem of correlations within a single biozone. As discussed in Veizer et al. (1997a) (their Fig. 8), the scatter of $^{87}Sr/^{86}Sr$ values at the Frasnian/Famenian transition, the Kellwasser 'event', results from real oscillations within one or two biozones. Yet, on larger regional or global scales, it is difficult to match these

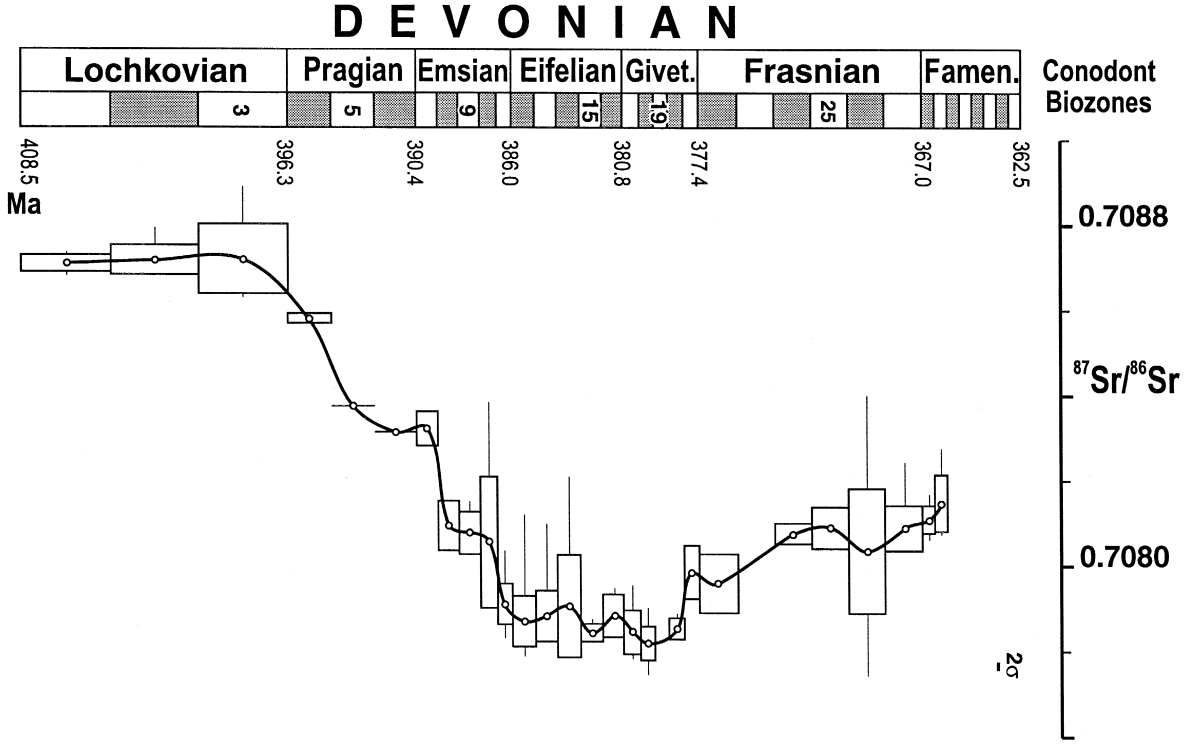

Fig. 6. $^{87}Sr/^{86}Sr$ variations during the Devonian based on conodont biozones. Explanations: circle = mean; box = $\pm 1\sigma$; vertical line = minimum and maximum. The 2σ in the lower right corner is an average 2σ for the NBS 987 standard. Note that only brachiopods are included in this figure. The biozones are the following (Weddige, 1977, 1988; Carls, 1988; Sandberg et al., 1989; Ziegler and Sandberg, 1990): 1 — *woschmidti*, 2 — *postwoschmidti*, 3 — *pesavis*, 4 — *sulcatus*, 5 — *kindleri*, 6 — *pirinea*, 7 — *deniscens*, 8 — *gronbergi*, 9 — *laticostatus*, 10 — *serotinus*, 11 — *patulus*, 12 — *partitus*, 13 — *costatus*, 14 — *australis*, 15 — *kockelianus*, 16 — *esensis* (*arkonensis*, *obliquimarginalus*, *bipecatus*), 17 — *hemiansatus*, 18 — *varcus*, 19 — *hermani* — *cristatus*, 20 — *disparitis*, 21 — *falsovialis*, 22 — *transitans*, 23 — *punctata*, 24 — *hassi*, 25 — *jamieae*, 26 — *rhenana*, 27 — *linguiformis*, 28 — *triangularis*, 29 — *crepida*, 30 — *rhomboidea*, 31 — *marginifera*, 32 — *trachytera*, 33 — *postera*, 34 — *expansa*, 35 — *presulcata*.

wiggles in different profiles. In effect, one is limited by constraints of biostratigraphy and the matching is in the term of biozones. This is not to say that some of the observed $^{87}Sr/^{86}Sr$ variations may not be a result of undetected post-depositional alteration, but a portion of these variations is real. It is therefore difficult to claim some specific $^{87}Sr/^{86}Sr$ value for a given biozone. The alternatives can rely on either selecting the least radiogenic value or accepting all 'good' data as representative of that biozone. We prefer the second approach as more representative of the real situation. We therefore plot the mean, the 2σ range and the total range of values for each of the 35 Devonian conodont biozones (Fig. 6). The Phanerozoic $^{87}Sr/^{86}Sr$ marine trend based on the above principles is, in our view, a more realistic reflection of the natural situation and as such should be constructed separately for each period, not only for the Devonian or Silurian (Azmy et al., 1999).

6. Correlation potential

Bearing in mind the above qualifications, Sr isotopes can serve as a useful complementary correlation tool, particularly for sequences where the biostratigraphic approach is of little value, due either to the dearth of fossils or to their limited stratigraphic utility. Nevertheless, the technique can lead to improved correlations even for sequences with good biostratigraphic control. Azmy et al. (1999) demonstrated that for the Silurian, the $^{87}Sr/^{86}Sr$ ratio enables stratigraphic assignment of samples from independent sets to within ± 1 graptolite biozones. This is no minor accomplishment considering the difficulty of correlation for profiles with differing sedimentation rates and taking into account the uncertainty of the 'first and last appearance' of a given 'Leitfossil' in the sedimentary record. The issue can be illustrated by the present study of the Givetian/Frasnian transition in the Eifel Mountains of Germany. These well-studied sections, in close proximity to the Belgian stratotypes, have a well-established biostratigraphy (Weddige, 1977; Struve, 1982). Unfortunately, the Givetian/Frasnian transition is strongly dolomitized and it was necessary to sample the coeval sections at the Teerstrassenbau Wahlheim/Friesenrath quarry in Aachen and at the tunnel near Behringhausen, east of the Rhine (Ostsauerland). The measured $^{87}Sr/^{86}Sr$ values (Fig. 7) define a rising trend of $\sim 3 \times 10^{-4}$ in about 4 Ma that spans the gap between the *varcus* (No. 18) and *rhenana* (No. 26) biozones in the Eifel. In detail, however, it appears that the steepest rise in the curve, of about

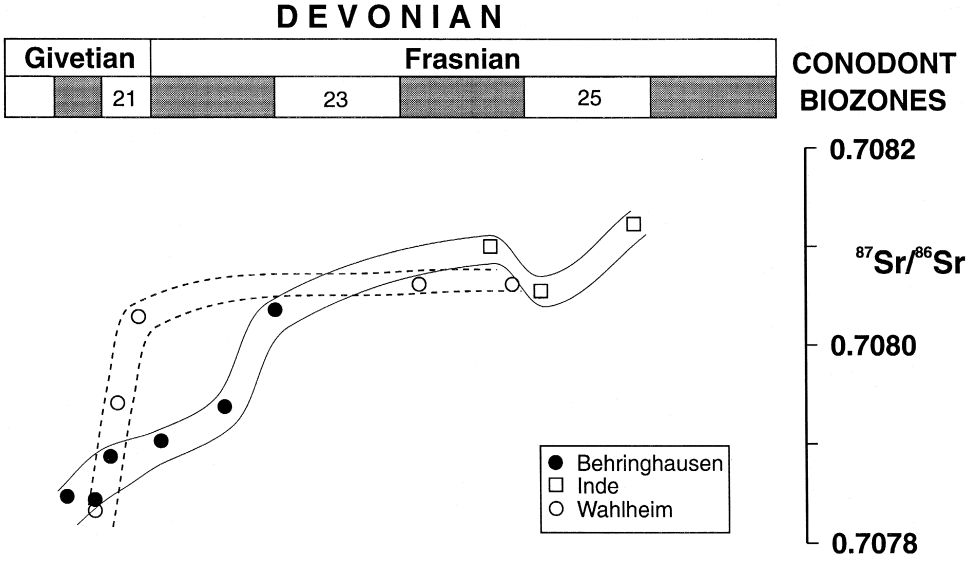

Fig. 7. $^{87}Sr/^{86}Sr$ trend at the Givetian/Frasnian transition. Conodont biozones as in Fig. 6.

1×10^{-4} in ≤ 1 Ma, appears in the *falsiovalis* (No. 21) conodont biozone in Aachen and in the *transitans* (No. 22) biozone in Behringhausen. The critical portion of the profile in Aachen is at its top (Reissner, 1990) and it was assigned to the (lower) *assymetricus* biozone in the older stratigraphic assignment (Ziegler, 1962) that encompassed the present *falsiovalis* and *transitans* biozones. If so, that portion of the Aachen profile that contained the brachiopods measured for $^{87}Sr/^{86}Sr$ should perhaps be assigned to the *transitans* biozone (No. 22), and be correlative with the Behringhausen.

A third approach of utilizing Sr isotopes for correlation purposes is based on inflexions in the trend (McArthur, 1994; Azmy et al., 1999). The higher-order oscillations are not necessarily reproducible, particularly in their amplitude. This is because the sedimentary sequences are not an unbroken recorder of time and the $^{87}Sr/^{86}Sr$ evolutionary trend of seawater can thus be truncated at any time prior to reaching the apex of an oscillation. An inflexion, on the other hand, can be recognized even if some corresponding strata are missing. Note that unrecognized hiatuses may appear also as abrupt 'jumps' in the strontium isotope trend (cf. Diener et al., 1996, their Fig. 7).

7. Phanerozoic $\delta^{13}C$ trend

The secular Phanerozoic trends based on the new Bochum/Ottawa dataset (Fig. 8) or on the compilation of literature data (Fig. 9) resemble each other in terms of their overall shape and in the considerable spread of values. As for Sr isotopes, some of this scatter is due to higher-order natural oscillations clumped together by compressed time scale. This is particularly the case for the literature dataset with its much poorer temporal resolution. Additional scatter

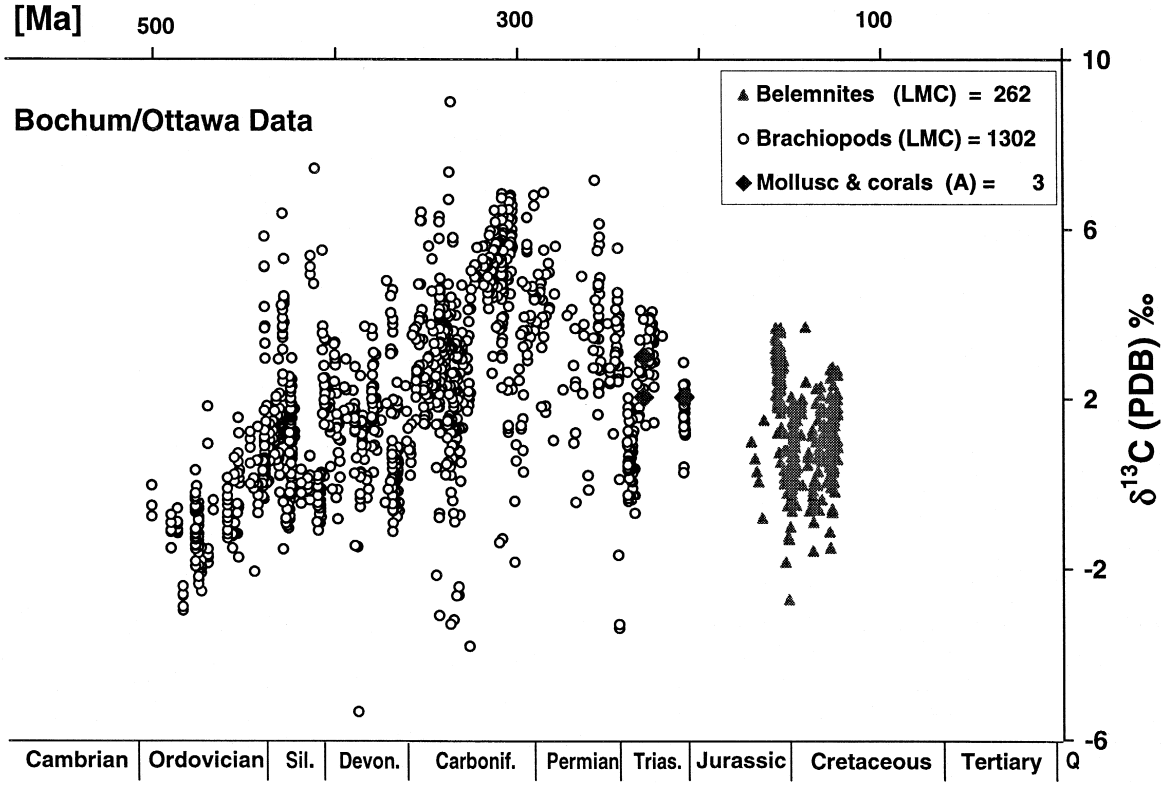

Fig. 8. Phanerozoic $\delta^{13}C$ trend based on 1564 brachiopod (secondary layer) and belemnite (laminae pelucidae) measurements at Bochum and Ottawa. Three Triassic samples (two corals and one bivalve) from Cassian Beds and Kössener Schichten (Alps) are still preserved as aragonite.

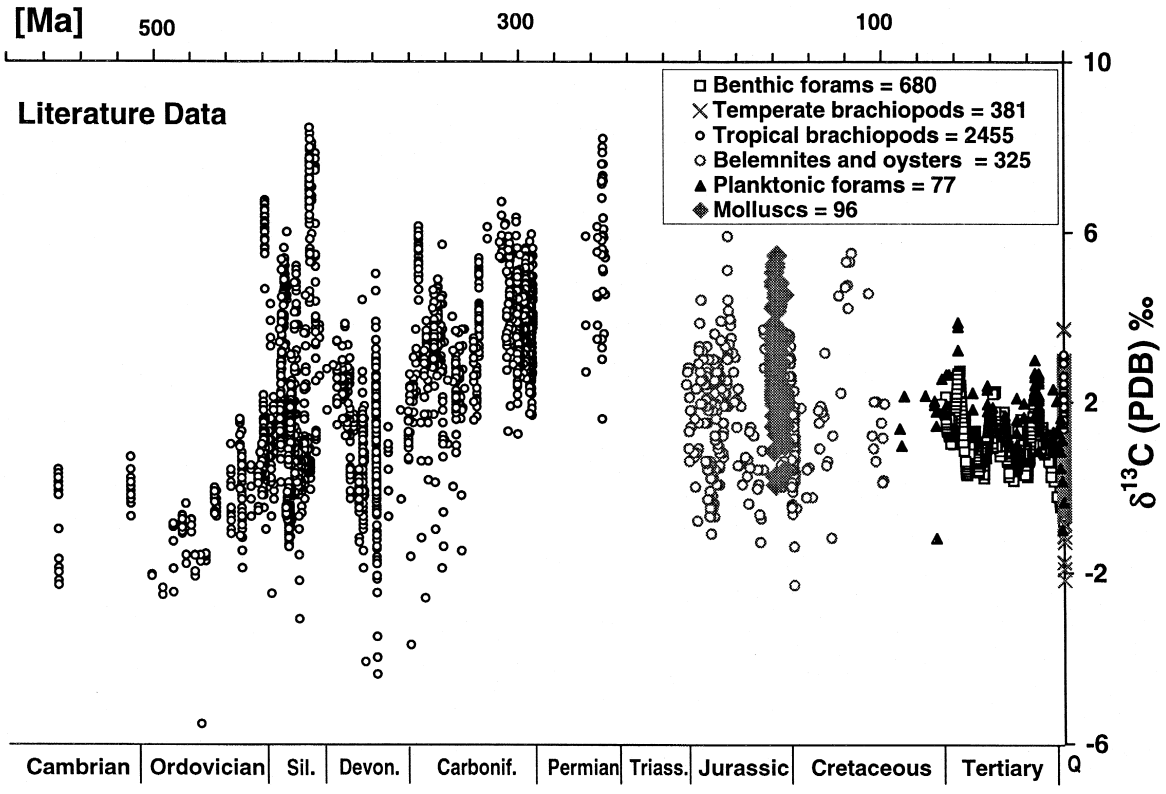

Fig. 9. Phanerozoic $\delta^{13}C$ trend compiled from 3918 measurements for LMC (brachiopods, belemnites, oysters, foraminifera) and 96 measurements for A (mollusc) shells. The sources of the data are the following: Compston (1960), Douglas and Savin (1971, 1973), Veizer and Hoefs (1976), Brand and Veizer (1981), Popp et al. (1986a,b), Veizer et al. (1986), Miller et al. (1987), Adlis et al. (1988), Brand (1989b), Delaney et al. (1989), Rush and Chafetz (1990), Grossman et al. (1991, 1993), Middleton et al. (1991), Jones (1992), Wadleigh and Veizer (1992), Brand and Legrand-Blain (1993), Lavoie (1993), Anderson et al. (1994), Qing and Veizer (1994), Carden (1995), Carpenter and Lohmann (1995), Mii (1996), Rao (1996), Samtleben et al. (1996), Wenzel and Joachimski (1996), James et al. (1997), Mii et al. (1997).

is due to oceanographic and biological factors, mentioned already in the introductory part, and well-preserved ancient aragonitic (Anderson et al., 1994) as well as modern calcitic representatives (Fig. 9) are no exception to this pattern. Both sets of data, as well as the secular $\delta^{13}C_{carbonate}$ curve based on whole rocks (Veizer et al., 1980; Lindh, 1983), show a general increase in $\delta^{13}C$ throughout the Paleozoic, followed by an abrupt decline and subsequent oscillations around the present-day value in the course of the Mesozoic and Cenozoic. Because of this coherence, we feel justified in pooling both datasets (Figs. 8 and 9) in order to generate a secular trend for the entire Phanerozoic (Fig. 10). The running mean based on this combined set was calculated for 5 Ma incremental shifts, because this is the realistic resolution for global biostratigraphic correlations and for our combined dataset. The bands around this mean incorporate 68 and 95% of all measured samples, respectively. Note also that superimposed on the overall trend are pronounced, but somewhat dampened due to the 20 Ma window, second- and higher-order oscillations. Considering the global nature of the database, with samples originating from five continents and a multitude of sedimentary basins, the observed peaks are likely of global significance. An exception may or may not be the Aptian peak at ~115 Ma that is based on a small number of measurements (cf. Podlaha et al., 1998). It is likely that even many of the shorter-term peaks may still be

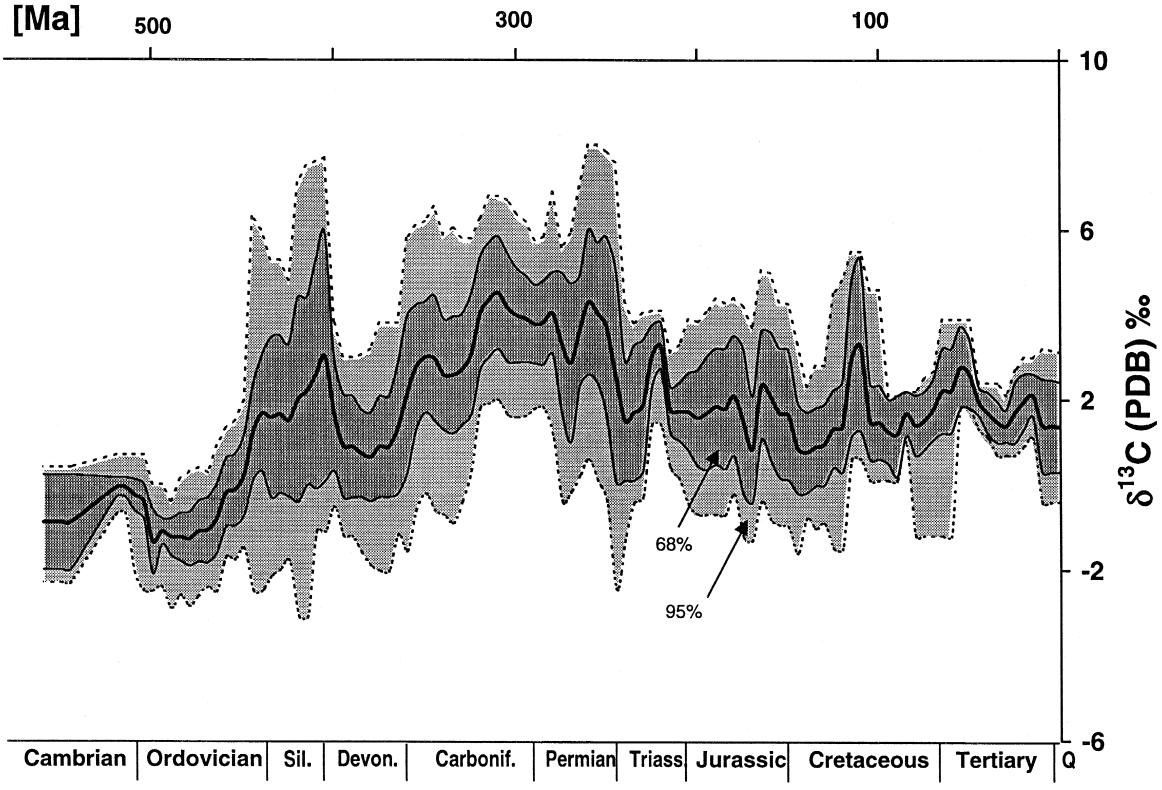

Fig. 10. Phanerozoic $\delta^{13}C$ trend for combined Bochum/Ottawa and literature data for LMC shells. The running mean is based on 20 Ma window and 5 Ma forward step. The shaded areas around the running mean include the 68% ($\pm 1\sigma$ for a strictly Gaussian distribution) and 95% ($\pm 2\sigma$) of all data.

of global significance, as will be discussed later for the terminal Ordovician.

8. Phanerozoic $\delta^{18}O$ trend

In analogy to carbon isotopes, the $\delta^{18}O$ trends for the Bochum/Ottawa (Fig. 11) and the literature datasets (Fig. 12) overlap, including their similarities in the second-order structure (e.g., the Silurian/Devonian dip followed by Carboniferous rise). We therefore feel justified in combining them into a general Phanerozoic trend (Fig. 13). Several features are immediately apparent from this presentation.

(1) The data define a trend of increasing $\delta^{18}O$ values, from about $-8‰$ at the onset of the Phanerozoic to about 0‰ at present.

(2) As for the $\delta^{13}C$, the trend is not a linear feature, but a band. Note, however, that the observed $\delta^{18}O$ variations in modern tropical brachiopods at shelf depths are $\sim 4‰$ (Carpenter and Lohmann, 1995; Bruckschen et al., 1999) and for the specimens from temperate climates they span about 8‰ (Fig. 12). A similar range of $\delta^{18}O$ values was observed by Anderson et al. (1994) for ancient belemnites and molluscs, the latter still preserved as pure aragonite (Fig. 13), within a single member of the Jurassic Oxford Clay Formation. From this perspective, it is indeed noteworthy that the collections of fossils from any one biozone, each representing populations with a much larger temporal and spatial range than the modern one, do not show a markedly larger dispersion of $\delta^{18}O$ values (Fig. 13). The existing ^{18}O depleted outliers in the Carboniferous and Permian (see Bruckschen et al., 1999 for further discussion) represent only $\sim 1\%$ of the total population, thus extending somewhat the lower range of the 95% limit. Such outliers have only a negligible impact on

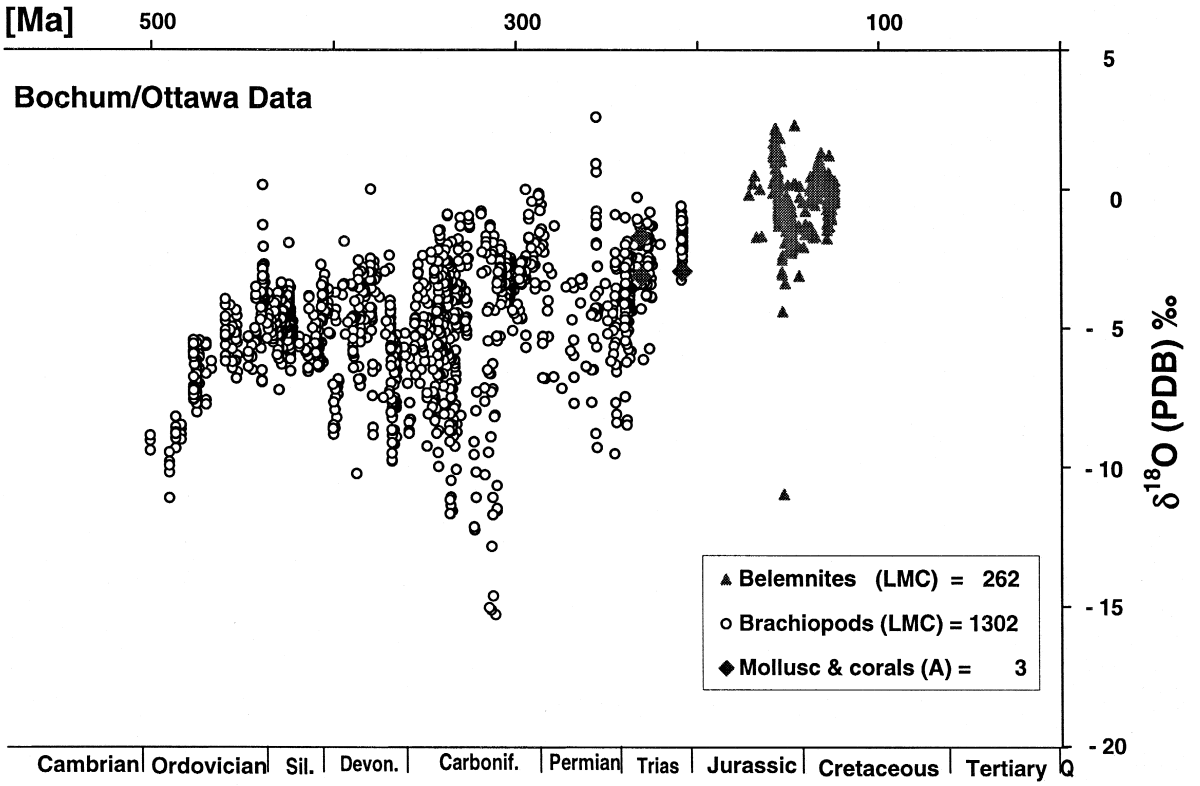

Fig. 11. Phanerozoic $\delta^{18}O$ trend based on 1654 brachiopod (secondary layer) and belemnite (laminae pellucidae) measurements at Bochum and Ottawa. Three Triassic mollusc samples are still preserved as aragonite (see Fig. 8).

the mean, the 2σ range, or the upper 95% boundary of the band. The latter boundary is sharp, with almost no samples above it (Figs. 11 and 12). Consequently, even an arbitrary retention of only the 'heaviest' values would not invalidate the secular Phanerozoic trend.

(3) Statistical treatment of the data (Fig. 13) suggests an existence of second-order oscillations with a frequency of $\sim$150 Ma, their apexes coincident with cold intervals and major glaciations. Advancing global cooling, intermittently compounded by generation of ice caps, could have been the principal reasons for the observed ^{18}O enrichments.

(4) The three Carboniferous molluscs entombed in asphalt and still well-preserved as nacreous aragonite (Brand, 1989a), as well as the 122 Jurassic and Triassic aragonitic molluscs (Anderson et al., 1994; Korte, 1999), all plot well within the main trend (Fig. 13).

All the above points will be of importance for discussion of the primary vs. secondary nature of the $\delta^{18}O$ Phanerozoic trend.

9. Correlation of oxygen and carbon isotopes

The crossplots of all Phanerozoic data (Fig. 14) show the relationships of $\delta^{18}O$ and $\delta^{13}C$ for the entire Phanerozoic. Covariant $\delta^{18}O/\delta^{13}C$ trends, such as those of the Ordovician, Silurian, Permian or Triassic, are often interpreted as an indicator of diagenetic resetting due to ^{18}O and ^{13}C depletion in altered samples (e.g., Bathurst, 1975). While post-depositional resetting, particularly in diagenetic systems dominated by bicarbonate generated from soil CO_2, can indeed generate such trends, their existence is not an a priori proof of diagenetic alteration. Modern shells, almost as a rule, display such positive

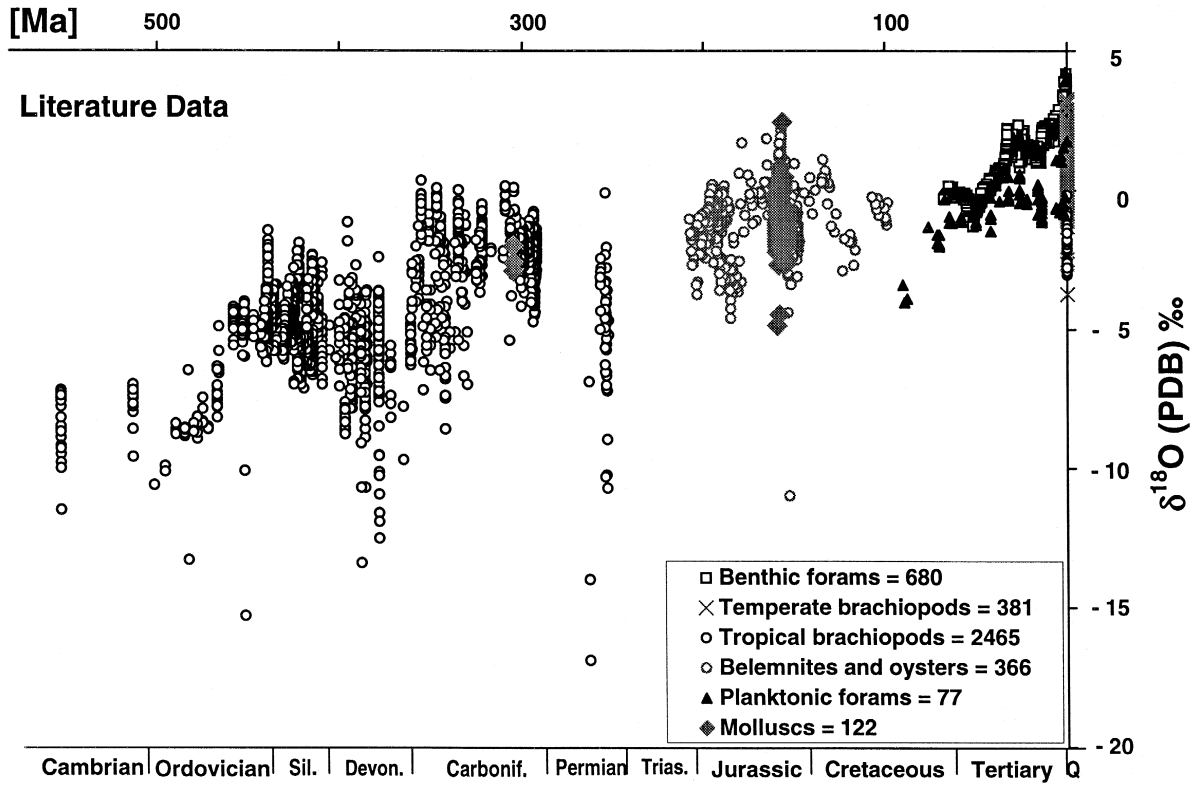

Fig. 12. Phanerozoic $\delta^{18}O$ trend of compiled 3969 measurements for LMC shells (brachiopods, belemnites, oysters, foraminifera) and 122 Carboniferous and Jurassic aragonitic mollusc shells (Brand, 1989a; Anderson et al., 1994), the latter listed in literature as 100% aragonite. The sources of the data are as in Fig. 9 and Lowenstam (1961).

covariance, principally due to isotope fractionation effects in the process of shell secretion (McConnaughey and Whelan, 1997). The pattern in the diagenetically unaffected Quaternary cluster (Fig. 14) confirms this assertion.

Another reason for the covariance, particularly during the Paleozoic, is the fact that both isotopes show a general secular increase with decreasing age. The Paleozoic cluster represents, therefore, with large degrees of overlap, a trend from the isotopically depleted Cambrian to the enriched Permian. In detail, the covariance is particularly pronounced for periods of fast secular change, such as the Ordovician. Note, however, that the patterns of this $\delta^{18}O/\delta^{13}C$ covariance shift toward positive $\delta^{18}O$ values with decreasing age. The spread of $\delta^{13}C$ values, on the other hand, remains relatively invariant.

In the late Paleozoic clusters, a number of samples fall outside the general covariance domain due to excessively negative $\delta^{18}O$ values. These samples, mostly of Carboniferous age, are the same that plot as ^{18}O depleted outliers in the $\delta^{18}O$ secular trend (Fig. 13). They originate mostly from the Donetsk Basin of the Ukraine and are further discussed in Bruckschen et al. (1999).

10. Primary or secondary trends

The primary nature of the $\delta^{13}C$ secular trend, at least in terms of its major features, is no longer disputed, but the issue is far from settled for the $\delta^{18}O$ (cf. Hoefs, 1997). Five lines of argumentation are pertinent to this issue: textural, geological, mineralogical, chemical and isotopic. We shall discuss them in this order.

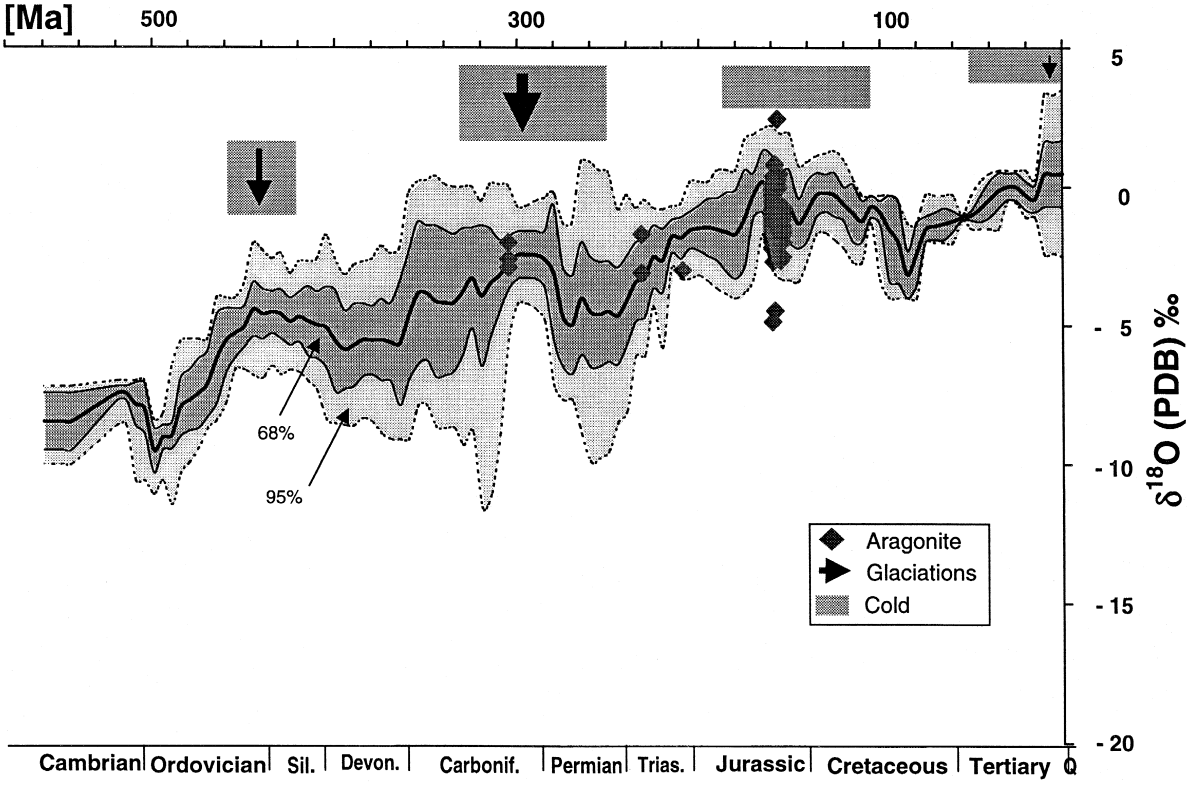

Fig. 13. Phanerozoic $\delta^{18}O$ trend for Bochum/Ottawa and literature data for LMC shells. Aragonite specimens as in Figs. 11 and 12. Note that benthic foraminifera are excluded from this figure, because they may not represent ecological analogues to ancient brachiopods and belemnites. Glaciations and cold times after Frakes et al. (1992). Further explanations as in Fig. 10.

Starting with the *textural considerations*, the excellent textural preservation of the shells, even on a sub-micron scale, is illustrated in Fig. 1 (cf. also Bruckschen et al., 1999). Such excellent preservation is by no means a rarity in the present dataset. Documentation can be found, e.g., in Brand (1989a,b), Wadleigh and Veizer (1992), Grossman et al. (1993), Qing and Veizer (1994), Carden (1995), Copper (1995), Azmy (1996), Grossman et al. (1996), Samtleben et al. (1996), Wenzel and Joachimski (1996), Wenzel (1997), Azmy et al. (1998) and others. Note that the depicted samples (Fig. 1) have trace element, $\delta^{13}C$ and $^{87}Sr/^{86}Sr$ values as expected for a Silurian marine calcite, yet their $\delta^{18}Os$ are around -5‰ PDB, well within the Phanerozoic trend (Fig. 13). For the sake of the argument, let us assume that the oxygen isotope values have been altered by meteoric waters with $\delta^{18}O$ of say -5 to -10‰ SMOW. In such a case, one-half to all of oxygens in these calcite structures, i.e., up to 60% of their building blocks, would have to be replaced by extraneous oxygen without leaving behind the slightest trace in the optical, mineralogical, chemical and isotopic make-up of the shells. This is difficult to conceive, irrespective of whether one invokes a solution/reprecipitation process or, the less likely, solid diffusion exchange.

The second line of argumentation is based on *geological consideration.* Let us assume that the trend of ^{18}O depletion with age (Fig. 13) is in the first instance a result of post-depositional resetting due to interaction with meteoric and/or warm waters. Diagenetic stabilization of carbonate rocks indeed results in ^{18}O depletion, but this depletion is mostly related to transformation of metastable polymorphs (aragonite, high-Mg calcite) into stable ones

(low-Mg calcite) and it usually happens very early in the post-depositional history of the rocks. Subsequently, and in deep sea environments, the alteration proceeds, at a slower rate, by pressure solution until complete lithification. Once lithified, the subsequent ^{18}O depletions — if any — are much less pronounced. Note also that all ancient carbonate rocks have undergone this stabilization step, thus self-correcting for it for rocks older than about Cenozoic. As a result, such a post-depositional trend would have a steep slope during the Cenozoic, exponentially flattening out with increasing age. Furthermore, due to vagaries of post-depositional development of different sedimentary basins, the resetting towards ^{18}O depleted values from the assumed modern day equilibrium would result in a fan-shaped pattern that broadens with age, with many outliers along the alteration pathway, i.e., between 0‰ PDB and the main Phanerozoic trend. Neither of these predictions is supported by experimental data (Figs. 11–13). Disregarding the second-order oscillations, the rate of decline is about linear, the band of about equal width, and *there are essentially no outliers above the upper limit of this band*. Whatever outliers do exist ($\sim$ 1% of samples), they plot mostly below the main trend, i.e., any post-depositional ^{18}O depletion advanced from (and not towards) the main trend. In order to sustain the diagenetic alternative, one would have to argue that the post-depositional alteration advances at roughly a constant rate, regardless of the age of the rocks, and that all basins throughout the world (see the distribution of our samples) have undergone alteration strictly proportional to their ages. Considering the plethora of geologic histories, with samples from all continents but Antarctica, and from a multitude of sedimentary basins, this is not a credible proposition.

As already pointed out, the apexes of the second-order oscillations appear to have coincided with cold periods (Fig. 13), perhaps indicating that the $\delta^{18}O$ oscillations reflect global cooling trends. Leaving aside the issue of the origin of these second-order oscillations, let us concentrate on one of them, the Ordovician/Silurian transition. The $\delta^{18}O$ record of this transition (Fig. 15) shows the $\delta^{18}O$ pattern (Carden, 1995; Azmy, 1996; Azmy et al., 1998) where the positive $\delta^{18}O$ excursions coincide, within the resolution of a biozone, with glacial sediments, a pattern, except for the shift in the baseline, analogous to that of the Quaternary. Furthermore, the pronounced terminal Ordovician $\delta^{18}O$ peak is clearly a global feature within the *acuminatus* (No. 21) biozone, because this signal was detected in China (Carden, this project), the Baltic region, Canada and Argentina (Brenchley et al., 1995; Marshall et al., 1997). This pattern can be easily understood in terms of the primary signal, but is difficult to reconcile with a diagenetic interpretation.

The third line of argumentation is based on the *mineralogy of the shells*. Because of their exceptionally well-preserved textures (Fig. 1), we believe that low-Mg calcitic shells were relatively resistant to diagenetic alteration. Moreover, molluscs that are still preserved in their highly unstable original aragonitic mineralogy also plot within the general trend defined by the low-Mg calcitic shells (Fig. 13). In order to sustain the diagenetic alternative, it would again be necessary to claim that all these shells exchanged most of their oxygen, yet retained not only their original low-Mg calcitic, but also original *aragonitic* mineralogies.

The fourth line of argumentation is based on the *chemical composition* of the studied samples. As already demonstrated (Fig. 2), a minimum of 2/3 of the 1370 samples studied by us for trace elements have compositions directly comparable to modern low-Mg calcitic shells. Diagenetic alterations usually lead to decline in Sr (Na) and increase in Mn (Fe) contents (Brand and Veizer, 1980; Veizer, 1983; Banner, 1995). Based on such criteria, about 1/3 of the samples characterized by Sr contents of less than about 800 ppm may arguably be considered somewhat altered. Nonetheless, trace element criteria for at least 2/3 of the samples are not consistent with the proposition of diagenetic alteration.

The fifth line of argumentation is based on the *isotopic patterns* of the studied populations. The present Phanerozoic dataset is the first of such quantity and quality where the samples have been studied simultaneously for $\delta^{18}O$, $\delta^{13}C$, $^{87}Sr/^{86}Sr$, trace elements, and optical parameters. In addition, some of the samples have been studied for $\delta^{34}S$ of structurally bound sulfur (Kampschulte and Strauss, 1996; Strauss, this issue). The possibility of a large stratigraphic mismatch for different isotopic systems is therefore mitigated. A crossplot of $\delta^{18}O$ vs. $^{87}Sr/^{86}Sr$

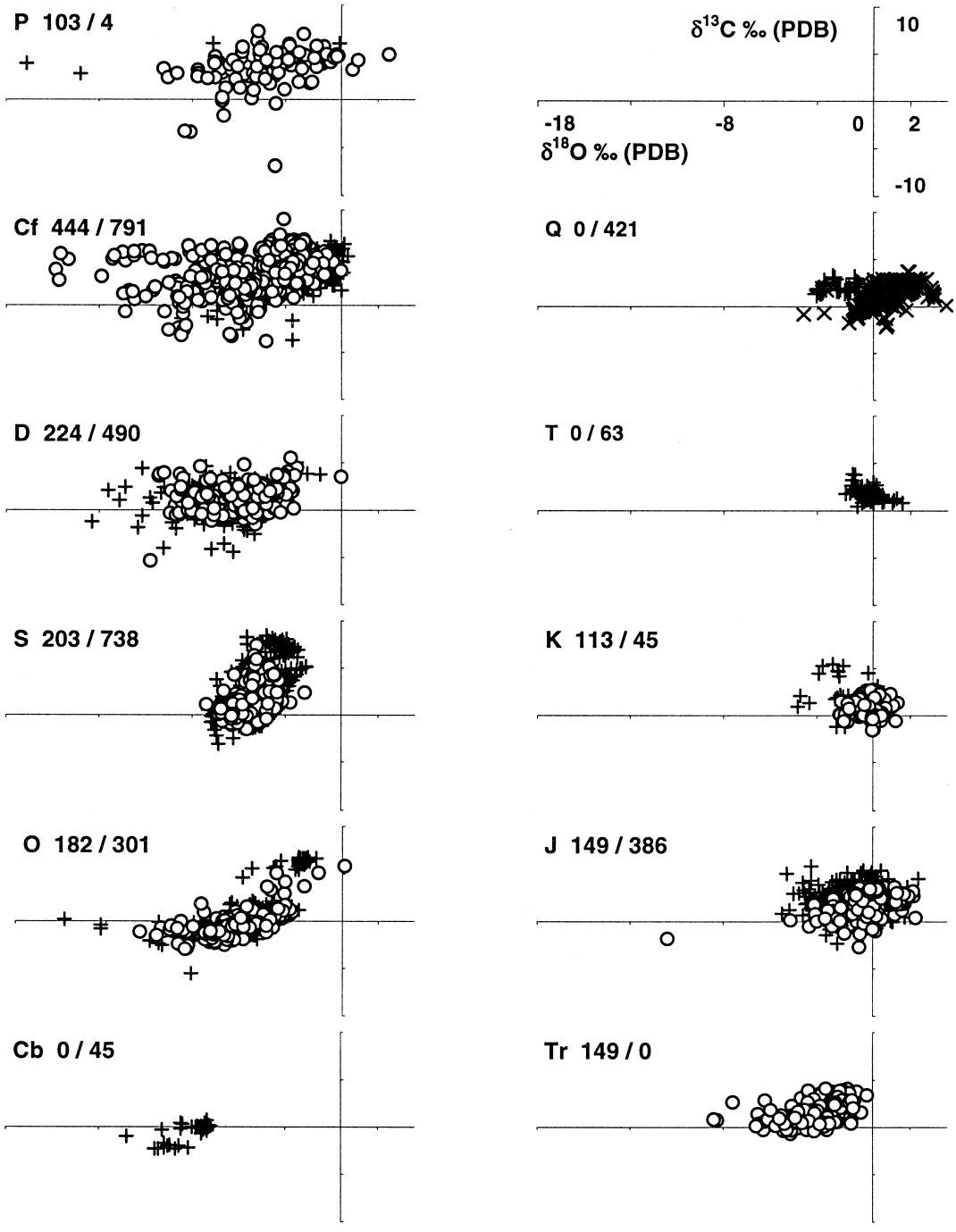

Fig. 14. The $\delta^{18}O$ vs. $\delta^{13}C$ crossplots for the samples listed in Figs. 9–12. Explanations: circles — Bochum/Ottawa data; upright crosses — literature data (LMC brachiopods, belemnites, oysters, foraminifera); diagonal crosses — literature data (LMC Quaternary temperate brachiopods). P 103/4: Permian, 103 Bochum/Ottawa samples/four literature samples. Note that the Tertiary field contains only pelagic foraminifera.

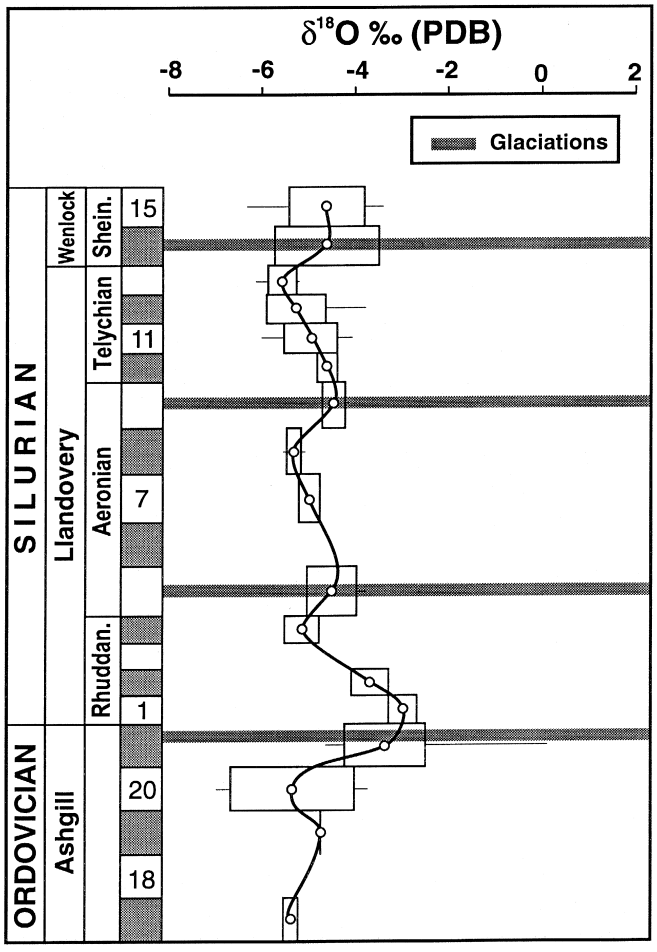

Fig. 15. The $\delta^{18}O$ trend across the Ordovician/Silurian transition. The Ordovician biozones, based on graptolites, are the following: 17 — *Pleugograptus linearis*, 18 — *Dicelograptus complanatus*, 19 — *Dic. anceps*, 20 — *Climacograptus extraordinarius*, 21 — *Glyptograptus acuminatus*. The Silurian graptolite biozones are the following: 1 — *Parakidograptus acuminatus*, 2 — *Atavograptus atavus*, 3 — *Lagarograptus acinaces*, 4 — *Coronograptus cyphus*, 5 — *Monograptus triangulatus*, 6 — *Diplograptus magnus*, 7 — *Pribylograptus leptotheca*, 8 — *Monog. convolutus*, 9 — *Monog. sedgwickii*, 10 — *Monog. turriculatus*, 11 — *Monog. crispus*, 12 — *Monoclimacis griestoniensis*, 13 — *Monoc. crenulata*, 14 — *Cyrtograptus centrifugus*, 15 — *Cy. murchisoni*. Glacial episodes after Grahn and Caputo (1992). Patterns as in Fig. 6.

(Fig. 16) shows a very high degree of correlation. From a purely theoretical perspective, one could perhaps argue that this correlation is a result of diagenetic alteration. In that case, however, the Sr isotopic trend (Fig. 4) would have to be a secondary feature as well. In order to escape such a conclusion, it would be necessary to postulate that the $^{87}Sr/^{86}Sr$ of some 4000 samples remained almost perfectly preserved (Fig. 4) while their oxygens have been heavily reset. This is not a credible proposition in view of the repeatedly documented reproducibility of the Sr isotope trend, even taking into account the differing water/rock ratios for these two elements in a diagenetic system.

Furthermore, all isotope pairs crosscorrelate (positively or negatively) at very high confidence levels (Fig. 17). We are not aware of any diagenetic scenario that would have been capable of producing such interrelationships. They can be, however, understood in terms of the primary signal that reflects

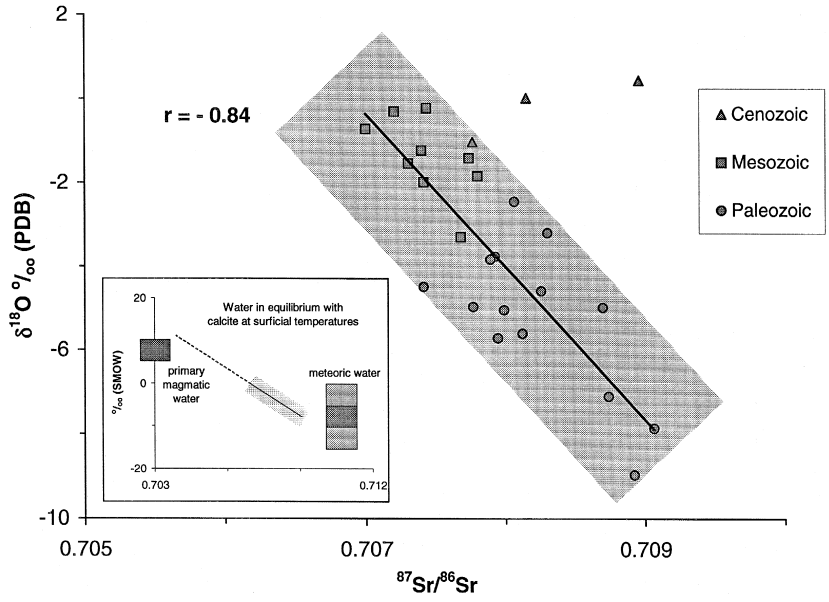

Fig. 16. Crossplot of mean $^{87}Sr/^{86}Sr$ vs. $\delta^{18}O$ values for 20 Ma intervals of the Phanerozoic. Mean values calculated from Figs. 4 and 13, respectively. The correlation coefficient is -0.57 for all points and -0.84 if the two Cenozoic points are excluded. Insert, based on the extension of the trend, suggests that seawater lies on a mixing line of two endmembers, primary magmatic water and meteoric water. The composition of endmembers from Hoefs (1997).

the operation of a unified and hierarchical exogenic system (litho-, hydro-, atmo-, biosphere) (Veizer, 1988), with tectonics driving it on geological time scales via its control of biogeochemical cycles, in this case the cycles of Sr, C, O and S. This proposition is supported by factor analysis (Table 2) which shows that the system is driven by three factors. The first factor links oxygen and strontium isotopic evolution (Fig. 16) and the second one $^{87}Sr/^{86}Sr$ and $\delta^{34}S$ (Fig. 18). These two factors explain up to 63% of the total variance. The last factor links the carbon and sulfur isotopic evolution (Fig. 19). Because of the high $^{87}Sr/^{86}Sr$ loadings, the tentative interpretation identifies the first two factors as tectonic, generated by the relative importance of the hydrothermal flux within the oceanic crust to its complementary meteoric component (riverine flux). The loading of sulfur and oxygen on two separate factors likely reflects the fact that the $^{18}O/^{16}O$ balance is temperature-dependent, with a crossover at $\sim 300°C$ (e.g., Gregory, 1991), while the $^{34}S/^{32}S$ is only marginally dependent on this variable. The third factor is a biologically mediated redox linkage of sulfur and carbon cycles (Garrels and Perry, 1974; Veizer et al., 1980). Considering that the ultimate goal of this contribution is to tackle the primary vs. secondary

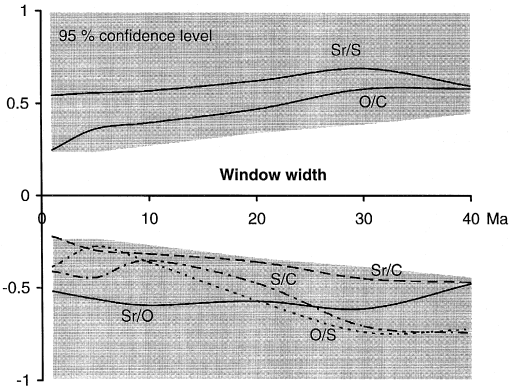

Fig. 17. Correlation coefficients for carbonate $^{87}Sr/^{86}Sr$, $\delta^{18}O$, $\delta^{13}C$ and sulfate $\delta^{34}S$ mean values during the Phanerozoic. The Sr, O and C isotope data from Figs. 4, 10 and 13, respectively. The $\delta^{34}S$ data from Strauss (1997, this issue). The means and their correlation coefficients have been calculated for 1 to 40 Ma intervals. The shading encloses the 95% confidence level domain.

Table 2
Factor analysis of $^{87}Sr/^{86}Sr$, $\delta^{13}C$, $\delta^{18}O$ and $\delta^{34}S$ for Phanerozoic seawater
The input data are 5 Ma averages from Figs. 4, 10 and 13 and from Strauss (1997, this issue), respectively. This resolution was selected because it represents the realistic stratigraphic resolution of our database. Note, however, that other reasonable resolutions (1–40 Ma) yield similar outcomes (cf. Fig. 17). Calculated without and with (in parentheses) the anomalous $^{87}Sr/^{86}Sr$ data for the last 35 Ma.

Variable	Factor 1	Factor 2	Factor 3
$^{87}Sr/^{86}Sr$	**−0.83 (−0.64)**	**0.55 (0.63)**	−0.06 (−0.05)
$\delta^{18}O$	**0.90 (0.75)**	−0.04 (−0.11)	0.31 (0.28)
$\delta^{34}S$	−0.15 (−0.11)	**0.77 (0.73)**	**−0.37 (−0.41)**
$\delta^{13}C$	0.17 (0.21)	−0.24 (−0.21)	**0.63 (0.65)**
Percent of variance explained	38.9 (25.7)	23.9 (24.8)	15.9 (16.8)

controversy for the $\delta^{18}O$ record, we prefer to refrain from further discussion of the subject. At this stage, we only wish to reiterate that the isotope data are not consistent with the diagenetic scenario.

The pattern in Fig. 16 shows that the latest ~35 Ma deviate from the overall correlation, suggesting that either the $\delta^{18}O$ or the $^{87}Sr/^{86}Sr$ of modern cycles are not in a steady state. Since this departure is visible only for Sr isotope data, it is likely that the Sr cycle is the culprit in terms of its isotopic composition. This may have a bearing on the controversy regarding the role of the Himalayas in the steep rise in $^{87}Sr/^{86}Sr$ of the Cenozoic seawater (Fig. 4). If the unroofing of the Himalayas were indeed the cause, the rise in seawater $^{87}Sr/^{86}Sr$ could have been accomplished either by an enhanced riverine Sr flux (Raymo and Ruddiman, 1992) and/or by its more radiogenic nature (Edmond, 1992). The isotopic relationships described in this contribution (Figs. 16–19) support the second alternative.

In the above discussion, we reviewed five lines of evidence for secondary vs. primary nature of the observed $\delta^{18}O$ secular trend. Our attempt to explain it as a secondary phenomenon failed, because it had to rely in all categories on a set of implausible and internally inconsistent special pleadings or could not be reconciled at all. The primary alternative, on the other hand, can be reconciled with all experimental observations. Note that we do not wish to claim that all samples are as well-preserved as those in Fig. 1. All screening techniques, singly or in concert, have their limitations and post-depositional alteration may indeed be partly responsible for some of the ^{18}O depleted 'troughs' in Fig. 13, such as the mid-

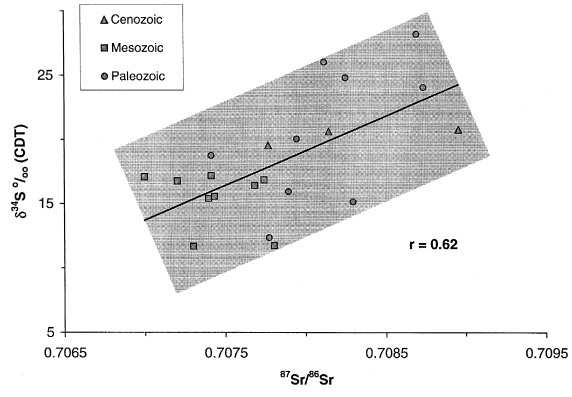

Fig. 18. Crossplot of mean $^{87}Sr/^{86}Sr$ and $\delta^{34}S$ values for 20 Ma intervals of the Phanerozoic. Mean values were calculated from Fig. 4 and Strauss (1997, (this issue), respectively. Note that the $\delta^{34}S$ data are those of evaporitic sulfates with their relatively poor temporal resolution.

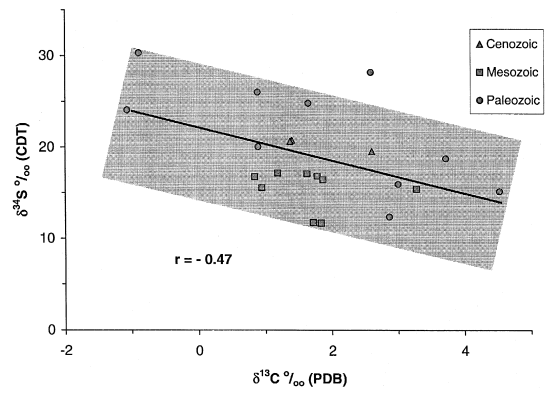

Fig. 19. Crossplot of mean $\delta^{13}C$ and $\delta^{34}S$ values for 20 Ma intervals of the Phanerozoic. Mean values were calculated from Fig. 10 and Strauss (1997, this issue), respectively. Note also that this factor is linked to the tectonic factor 2 via its sulfur and not the carbon cycle (Table 2).

Carboniferous. Nonetheless, except for these outliers, the cumulative optical, geological, mineralogical, chemical and isotopic evidence for the primary nature of the Phanerozoic secular $\delta^{18}O$ trend, at least in its major features, is compelling.

For the sake of a rounded discussion, we also consider two *objections* frequently raised against the primary nature of the $\delta^{18}O$ secular trend.

(1) The brachiopods define a secular trend that overlaps with that of the whole rocks, the latter undoubtedly isotopically reset (Land, 1995).

(2) The studies of oceanic crust and of ophiolites (e.g., Muehlenbachs and Clayton, 1976; Gregory and Taylor, 1981) suggest that the magnitudes of high- and low-temperature hydrothermal processes along their depth profile are about equal and thus cancel their opposing impact on the $\delta^{18}O$ of circulating water. As a result, the seawater $\delta^{18}O$ is, and has been, buffered around its present day value of about 0‰ SMOW (Gregory, 1991).

Concerning the first point, we already argued that diagenetic stabilization of *shelf carbonate facies* is mostly related to transformation of metastable polymorphs (aragonite, high-Mg calcite) into stable ones (low-Mg calcite) and usually happens very early in the post-depositional history of the rocks, at times when diagenetic solutions still retain partial memory of their seawater precursors (Choquette and James, 1990; James and Choquette, 1990). This often limits the whole rock shift to about -2‰ (Fig. 20). Once stabilized, the subsequent ^{18}O depletions are much less pronounced. Such a shift can well be accommodated within the $\delta^{18}O$ secular band, particularly since the major rock components, the micritic matrix and the early, marine, cements, had initial $\delta^{18}O$ compositions around and above the top boundary (e.g., Milliman, 1974; Bathurst, 1975; Tucker and Wright, 1990) of the band based on skeletal precipitates.

Additional support for the claim that the bulk of diagenetic stabilization of shelf carbonates usually ceases at a rather early stage of diagenetic history is provided by sulfur isotope data. Kampschulte and Strauss (1998) studied the $\delta^{34}S$ of trace sulfate from brachiopods and their host rocks from this same Bochum/Ottawa collection. The $\delta^{34}S$ of the shells, as well as of the host rocks, all plot on the Phanerozoic $\delta^{34}S$ secular trend for evaporites. Such coherence can only be generated if the system 'shuts down' at a very early diagenetic stage, at times when pore waters still retain the memory of seawater composition.

Apart from the argument for the early diagenetic overprint, we wish to point out the misunderstandings that frequently arise from model images of

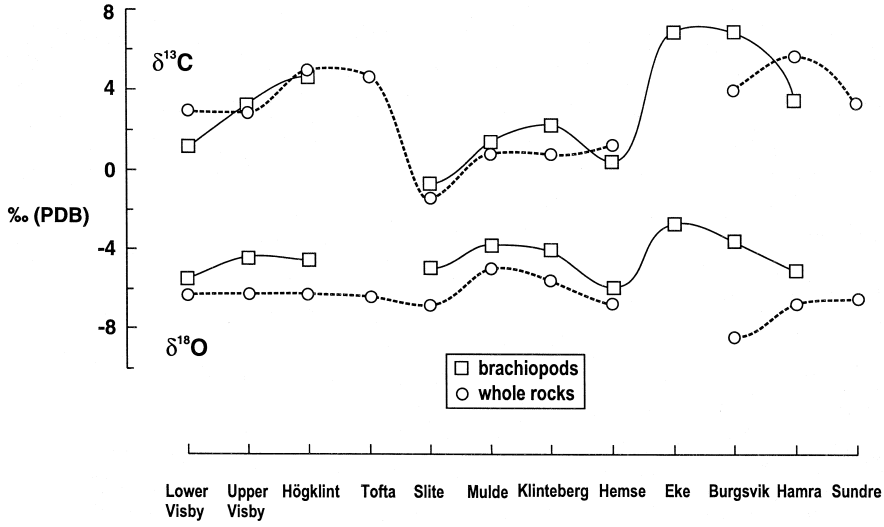

Fig. 20. The average formational $\delta^{13}C$ and $\delta^{18}O$ for the Silurian strata at Gotland. The brachiopod data are from Wenzel (1994) and the whole rock data from Jux and Steuber (1992). Note that except for the Burgsvik Formation that contains a disproportionate share of late meteoric cements, the $\delta^{13}C$ means are comparable, while the $\delta^{18}O$'s of whole rocks are depleted consistently by ~ 2‰ relative to brachiopods. Courtesy of W. Buggisch and B. Wenzel.

diagenesis. The reigning models of bulk rock solution/precipitation, diffusion/advection type (e.g., Richter and DePaolo, 1987; Schrag, this issue) have only limited applicability for diagenesis of *multi-component* carbonate assemblages. These models, like their groundwater flow system precursors en vogue for the shelf facies in the 1960s and 1970s, predict well the chemical and isotopic gradients in pore waters, but not the chemistry of the diverse solid phases. The reason is that only a minuscule portion of the solids is required to generate the pore water gradients. Yet, it is not the millionth portion of every particle that reacts, at any instant, with the water, but only the most soluble millionth particle. This is repeated with the next most soluble particle, etc. As a result, the stabilized bulk rock consists of domains that may have been completely, even repeatedly, recrystallized, while neighbouring domains could have remained practically unscathed (cf. Brand and Veizer, 1980). This is the reason for the excellent textural, chemical and isotopic preservation of some components, such as the presently studied LMC shells.

Concerning the second argument, we concur that the oceanic ridge circulation (Muehlenbachs and Clayton, 1976; Gregory, 1991) is the, or one of several, controlling factor of $\delta^{18}O$ composition of seawater. Accepting this, the Phanerozoic trend can be reproduced, providing the magnitude of high-temperature alteration is kept consistently higher than that of its low-temperature analogue (Fig. 21). Modification of the 'balanced' model could therefore be a solution to the dilemma. Theoretically, the required imbalance could be created by either assigning a greater magnitude to the high-T flux or a lesser one to the low-T flux. The former may result from processes within the oceanic crust itself, such as those that generate the ^{18}O depleted gabbros (Lecuyer and Reynard, 1996), or at magma chambers of subduction domains. Alternatively, the diminished low-T flux may be a consequence of a decline in continental weathering input.

A corollary to this argument is the claim that alteration trends in ophiolites 'prove' the buffering of $\delta^{18}O$ of ancient seawater at near modern values. In reality, these trends prove only that the waters were depleted in ^{18}O relative to the mineral assemblages of the ophiolites. At this stage, considering

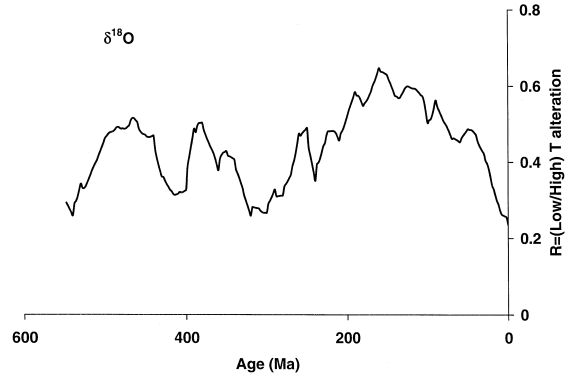

Fig. 21. Theoretical model of hydrothermal alteration required to produce the entire $\delta^{18}O$ secular trend in terms of changing sea water $^{18}O/^{16}O$ ratios. The model calculated evolution of the ratio R between the ^{18}O flux consumed by the weathering of seafloor basalts at low temperature and the ^{18}O flux produced by the high temperature weathering that is needed to reproduce an increase of about 8‰ in the $\delta^{18}O$ of seawater over the Phanerozoic. The curve was obtained by using a modified version of the ICM model (Goddéris and François, 1996), including the global alkalinity, carbon, $\delta^{18}O$, $\delta^{13}C$ and $^{87}Sr/^{86}Sr$ budgets. The result indicates that the R should be about 40–50% in the course of the Phanerozoic. Continental contribution to the oxygen cycle was also taken into account.

the large scatter in the alteration patterns, we are neither in a position to demonstrate unequivocally the equality of the low- and high-temperature fluxes, nor to differentiate between alteration halos generated by water with $\delta^{18}O$ of 0‰ instead of say -5‰ SMOW.

We wish to emphasize that despite all the above argumentation, we do not suggest that the entire observed $\delta^{18}O$ secular trend would have to be accommodated by changes in isotopic composition of ancient seawater (cf. Azmy et al., 1998). At this stage, we only advocate a reassessment of discrepancies between theory and experimental data, an alternative far preferable to the wholesale dismissal of the latter.

11. Conclusions

Optical, mineralogical, chemical and isotopic studies of a large collection of newly sampled Phanerozoic low-Mg calcitic fossils (brachiopods and belemnites), complemented by geological considera-

tions, demonstrate that the bulk of the shells are well-preserved and likely retained their primary isotope signals. The newly generated $^{87}Sr/^{86}Sr$ curve based on low-Mg fossils and conodonts resembles the one by Burke et al. (1982), but with greater detail and less dispersion.

The $\delta^{13}C$ curve for the Phanerozoic shows a general increase from about $-1 \pm 1‰$ to $+4 \pm 2‰$ PDB during the Paleozoic, an abrupt drop of 2‰ at the Permian/Triassic transition and oscillations around $+2‰$ in the course of the Mesozoic and Cenozoic. Superimposed on this general trend are higher-order oscillations, dominantly of global significance.

The $\delta^{18}O$ shows a general increase from about $-8‰$ to 0‰ PDB in the course of the Phanerozoic. Superimposed on this overall trend are second-order oscillations of ~ 150 Ma duration, their apexes coincident with cold intervals.

The means of Phanerozoic $^{87}Sr/^{86}Sr$, $\delta^{13}C$, $\delta^{18}O$ and $\delta^{34}S_{sulfate}$ correlate at any resolution in excess of 1 Ma, suggesting that we are dealing with a unified exogenic system (litho-, hydro-, atmo-, biosphere) driven by tectonic forces. Factor analysis shows that the above variables are controlled by three factors. The first factor is characterized by reciprocal loadings of $^{87}Sr/^{86}Sr$ and $\delta^{18}O$, the second by positive loadings of $^{87}Sr/^{86}Sr$ and $\delta^{34}S$, and the third one by reciprocal loadings of $\delta^{34}S$ and $\delta^{13}C$. We interpret the first two factors as tectonic and the third one as a biologically mediated redox balance of carbon and sulfur cycles.

Acknowledgements

This study has been supported financially by the Deutsche Forschungsgemeinschaft (particularly by the endowment from the G.W. Leibniz Prize to Jan Veizer) and by the Natural Sciences and Engineering Research Council of Canada. Financial support of the Canadian Institute for Advanced Research, through its 'Earth System Evolution' program, enabled extensive exchange of ideas with coparticipants. The establishment of the NSERC/Noranda/CIAR 'Earth System' Industrial Research Chair at the University of Ottawa partially freed J. Veizer from daily responsibilities. In addition, G.G. Hatch provided financial support for the isotope laboratories. We thank U. Brand, W. Buggisch, S.J. Carpenter, H.S. Chafetz, E.L. Grossman, J.D. Hudson, H.-S. Mii, N.B. Popp, B. Wenzel and J. Zachos for help with acquisition of literature data, P. Wickham for technical assistance, and J. Hoefs, J.D. Hudson and L.P. Knauth for review of the manuscript.

References

Adlis, D.S., Grossman, E.L., Yancey, T.E., McLerran, D.R., 1988. Isotope stratigraphy and paleodepth changes of Pennsylvanian cyclical sedimentary deposits. Palaios 3, 487–506.

Ala, D., 1996. High resolution isotope stratigraphy of the Lower Devonian. MSc thesis, University of Ottawa, Ottawa, Canada.

Algeo, T.J., Wilkinson, B.H., 1988. Periodicity of mesoscale Phanerozoic sedimentary cycles and the role of Milankovitch orbital modulation. J. Geol. 96, 313–322.

Anders, M.H., Krueger, S.W., Sadler, P.M., 1987. A new look at sedimentation rates and the completeness of the stratigraphic record. J. Geol. 95, 1–14.

Anderson, T.F., Popp, B.N., Williams, A.C., Ho, L.-Z., Hudson, J.D., 1994. The stable isotopic record of fossils from the Peterborough Member, Oxford Clay Formation (Jurassic), UK: paleoenvironmental implications. J. Geol. Soc. London 151, 125–138.

Arthur, M.A., Dean, W.E., Schlanger, S.O., 1985. Variations in the global carbon cycle during the Cretaceous related to climate, volcanism, and changes in atmospheric CO_2. Geophys. Monogr. 32, 504–529.

Azmy, K., 1996. Isotopic composition of Silurian brachiopods: implications for coeval seawater PhD Thesis, University of Ottawa, Ottawa, Canada.

Azmy, K., Veizer, J., Bassett, M.G., Copper, P., 1998. Oxygen and carbon isotopic composition of Silurian brachiopods: implications for seawater isotopic composition and glaciation. Geol. Soc. Am. Bull. 110, 1499–1512.

Azmy, K., Veizer, J., Wenzel, B., Bassett, M.G., Copper, P., 1999. Silurian strontium isotope stratigraphy. Geol. Soc. Am. Bull. 111, 475–483.

Baertschi, P., 1957. Messung und Deutung relativer Häufigkeitsvariationen vom O^{18} und C^{13} in Karbonatgesteinen und Mineralien. Schweiz. Mineral. Petrogr. Mitt. 37, 73–152.

Banner, J.L., 1995. Application of the trace element and isotope geochemistry of strontium to studies of carbonate diagenesis. Sedimentology 42, 805–824.

Banner, J.L., Hanson, G.N., 1990. Calculation of simultaneous isotopic and trace element variations during water–rock interaction with application to carbonate diagenesis. Geochim. Cosmochim. Acta 54, 3123–3138.

Banner, J.L., Kaufman, J., 1994. The isotopic record of ocean chemistry and diagenesis preserved in non-luminescent brachiopods from Mississippian carbonate rocks, Illinois and Missouri. Geol. Soc. Am. Bull. 106, 1074–1082.

Barrera, E., Baldauf, J., Lohmann, K.C., 1993. Strontium isotope and benthic foraminifer stable isotope results from Oligocene sediment at site 803. Proc. ODP, Sci. Res. 130, 269–279.

Bathurst, R.G.C., 1975. Carbonate Sediments and their Diagenesis. Elsevier, Amsterdam.

Berner, R.A., 1994. GEOCARB II: a revised model of atmospheric CO_2 over Phanerozoic time. Am. J. Sci. 294, 56–91.

Berner, R.A., Lasaga, A.C., Garrels, R.M., 1983. The carbonate–silicate geochemical cycle and its effect on atmospheric carbon dioxide over the past 100 million years. Am. J. Sci. 283, 641–683.

Bertram, C.J., Elderfield, H., Aldridge, R.J., Morris, S.C., 1992. $^{87}Sr/^{86}Sr$, $^{143}Nd/^{144}Nd$ and REEs in Silurian phosphatic fossils. Earth Planet. Sci. Lett. 113, 239–249.

Bowring, S.A., Erwin, D.H., 1998. A new look at evolutionary rates in deep time: uniting paleontology and high-precision geochronology. GSA Today 8, 1–8.

Brand, U., 1989a. Aragonite–calcite transformation based on Pennsylvanian molluscs. Geol. Soc. Am. Bull. 101, 377–390.

Brand, U., 1989b. Biogeochemistry of late Paleozoic North American brachiopods and secular variation of seawater composition. Biogeochemistry 7, 159–193.

Brand, U., 1991. Strontium isotope diagenesis of biogenic aragonite and low-Mg calcite. Geol. Soc. Am. Bull. 101, 377–390.

Brand, U., Legrand-Blain, M., 1993. Paleoecology and biogeochemistry of brachiopods from the Devonian–Carboniferous boundary interval of the Griotte Formation, La Serre, Montagne Noire, France. Ann. Soc. Géol. Belg. 115, 497–505.

Brand, U., Veizer, J., 1980. Chemical diagenesis of a multicomponent carbonate system: 1. Trace elements. J. Sediment. Petrol. 50, 1219–1236.

Brand, U., Veizer, J., 1981. Chemical diagenesis of a multicomponent carbonate system: 2. Stable isotopes. J. Sediment. Petrol. 50, 987–997.

Brass, G.W., 1976. The variation of the marine $^{87}Sr/^{86}Sr$ ratio during Phanerozoic time: interpretation using a flux model. Geochim. Cosmochim. Acta 40, 721–730.

Brass, G.W., Southam, J.R., Peterson, W.N., 1982. Warm saline bottom water in the ancient ocean. Nature 296, 620–623.

Brenchley, P.J., Carden, G.A.F., Marshall, J.D., 1995. Environmental changes associated with the 'first strike' of the late Ordovician mass extinction. Mod. Geol. 20, 69–82.

Bruckschen, P., Veizer, J., 1997. Oxygen and carbon isotopic composition of Dinantian brachiopods: paleoenvironmental implications for the Lower Carboniferous of western Europe. Paleogeogr., Paleoclimatol., Paleoecol. 132, 243–264.

Bruckschen, P., Bruhn, F., Meijer, J., Stephan, A., Veizer, J., 1995a. Diagenetic alteration of calcitic fossil shells: proton microprobe (PIXE) as a trace element tool. Nucl. Instrum. Methods Phys. Res. B 104, 427–431.

Bruckschen, P., Bruhn, F., Veizer, J., Buhl, D., 1995b. $^{87}Sr/^{86}Sr$ isotope evolution of the Lower Carboniferous seawater: Dinantian of western Europe. Sediment. Geol. 100, 63–81.

Bruckschen, P., Oesmann, S., Veizer, J., 1999. Isotope stratigraphy of the European Carboniferous: proxy signals for ocean chemistry, climate and tectonics. Chem. Geol. 161, 127–163.

Bruhn, F., 1995. Kombinierte Spurenelement-Mikroanalysen und Kathodolumineszenz-Untersuchungen: Entwicklung einer Messmethodik für die Bochumer Protonenmikrosonde (PIXE) und Fallstudien aus der Sedimentologie. RNDr Thesis, Ruhr–Universität, Bochum, Germany.

Bruhn, F., Bruckschen, P., Richter, D.K., Meijer, J., Stephan, A., Veizer, J., 1995. Diagenetic history of sedimentary carbonates: constraints from combined cathodoluminescence and trace element analyses by micro-PIXE. Nucl. Instrum. Methods Phys. Res. B 104, 409–414.

Bruhn, F., Korte, C., Meijer, J., Stephan, A., Veizer, J., 1997. Trace element concentrations in conodonts measured by the Bochum proton microprobe. Nucl. Instrum. Methods Phys. Res. B 130, 630–640.

Burke, W.H., Denison, R.E., Hetherington, E.A., Koepnick, R.B., Nelson, H.F., Otto, J.B., 1982. Variation of seawater $^{87}Sr/^{86}Sr$ throughout Phanerozoic time. Geology 10, 516–519.

Carden, G.A.F., 1995. Stable isotopic changes across the Ordovician–Silurian boundary. PhD Thesis, Univ. of Liverpool, Liverpool, England.

Carls, P., 1988. The Devonian of Celtiberia (Spain) and Devonian paleogeography of SW Europe. In: McMillan, M.J., Embry, A.F., Glass, D.J. (Eds.), Devonian of the World. Mem. Can. Soc. Petrol. Geol., Vol. 14, pp. 421–466.

Carpenter, S.J., Lohmann, K.C., 1995. $\delta^{18}O$ and $\delta^{13}C$ values of modern brachiopods. Geochim. Cosmochim. Acta 59, 3749–3764.

Chaisi, S.D., Schmitz, B., 1995. Stable ($\delta^{13}C$, $\delta^{18}O$) and strontium ($^{87}Sr/^{86}Sr$) isotopes through the Paleocene at Gebel Aweina, eastern Tethyan region. Paleogeogr., Paleoclimatol., Paleoecol. 116, 103–129.

Choquette, P.W., James, N.P., 1990. Limestones — the burial diagenetic environment. In: McIlreath, I.A., Morrow, D.W. (Eds.), Diagenesis. Geosci. Can. Repr. Ser., Vol. 4, pp. 75–112.

Clayton, R.M., Degens, E.T., 1959. Use of C isotope analyses for differentiating freshwater and marine sediments. AAPG Bull. 42, 890–897.

Coleman, M.L., Walsh, J.N., Benmore, R.A., 1989. Determination of both chemical and stable isotope composition in milligram-size carbonate samples. Sediment. Geol. 65, 233–238.

Compston, W., 1960. The carbon isotopic composition of certain marine invertebrates and coals from the Australian Permian. Geochim. Cosmochim. Acta 18, 1–22.

Copper, P., 1995. Five new genera of Late Ordovician–early Silurian brachiopods from Anticosti Island, eastern Canada. J. Paleontol. 69, 846–862.

Cummins, D.I., Elderfield, H., 1994. The strontium isotopic composition of Brigantian/late Dinantian seawater. Chem. Geol. 118, 255–270.

Dash, E.J., Biscaye, P.E., 1971. Isotope composition of strontium in Cretaceous–Recent pelagic foraminifera. Earth Planet. Sci. Lett. 11, 201–204.

Degens, E.T., Epstein, S., 1962. Relationship between $^{18}O/^{16}O$ ratios in coexisting carbonates, cherts and diatomites. Am. Assoc. Petrol. Geol. Bull. 46, 534–542.

Delaney, M.L., Popp, B.N., Lepzelter, C.G., Anderson, T.F., 1989. Lithium-to-calcium ratios in modern Cenozoic, and

Paleozoic articulate brachiopod shells. Paleoceanography 4, 681–691.

Denison, R.E., Koepnick, R.B., Burke, W.H., Hetherington, E.A., Fletcher, A., 1994. Construction of the Mississipian, Pennsylvanian and Permian seawater $^{87}Sr/^{86}Sr$ curve. Chem. Geol. Isot. Geosci. Sect. 112, 145–167.

DePaolo, D.J., Ingram, B.L., 1985. High-resolution stratigraphy with strontium isotopes. Science 227, 938–941.

Derry, L.A., Kaufman, A.J., Jacobsen, S.B., 1992. Sedimentary cycling and environmental change in the Late Proterozoic: evidence from stable and radiogenic isotopes. Geochim. Cosmochim. Acta 56, 1317–1329.

Dia, A.N., Cohen, A.S., O'Nions, R.K., Shackleton, N.J., 1992. Seawater Sr isotope variation over the past 300 kyr and influence of global climate cycles. Nature 356, 786–788.

Diener, A., 1991. Variationen im Verhältnis von $^{87}Sr/^{86}Sr$ in Brachiopodenschalen aus dem Devon der Eifel. Diplom Arbeit, Ruhr-Universität, Bochum, Germany.

Diener, A., Ebneth, S., Veizer, J., Buhl, D., 1996. Strontium isotope stratigraphy of the middle Devonian: brachiopods and conodonts. Geochim. Cosmochim. Acta 60, 639–652.

Dingus, L., 1984. Effects of stratigraphic completeness on interpretations of extinction rates across the Cretaceous–Tertiary boundary. Paleobiology 10, 420–438.

Douglas, R.G., Savin, S.M., 1971. Isotopic analysis of planktonic foraminifera from the Cenozoic of northwest Pacific, Leg 6. Init. Rep. Deep See Drill. Proj. 6, 1123–1127.

Douglas, R.G., Savin, S.M., 1973. Oxygen and carbon isotope analyses of Cretaceous and Tertiary foraminifera from Central North Pacific. Init. Rep. Deep Drill. Proj. 17, 591–605.

Ebneth, S., 1991. Variationen im Verhältnis von $^{87}Sr/^{86}Sr$ in Conodonten aus dem Devon der Eifel. Diplom Arbeit, Ruhr-Universität, Bochum, Germany.

Ebneth, S., Diener, A., Buhl, D., Veizer, J., 1997. Strontium isotope systematics of conodonts: Middle Devonian, Eifel Mountains, Germany. Paleogeogr., Paleoclimatol., Paleoecol. 132, 79–96.

Edmond, J.M., 1992. Himalayan tectonics, weathering processes and the strontium isotope record in marine limestones. Science 258, 1594–1597.

Elderfield, H., 1986. Strontium isotope stratigraphy. Paleogeogr., Paleoclimatol., Paleoecol. 57, 71–90.

Farrell, J.W., Clemens, S.C., Gromet, L.P., 1995. Improved chronostratigraphic reference curve of late Neogene seawater $^{87}Sr/^{86}Sr$. Geology 23, 403–406.

Faure, G., 1986. Principles of Isotope Geology. Wiley, New York.

Fauville, A., 1995. Der Nachweis der analytischen und stratigraphischen Reproduzierbarkeit von Strontiumisotopenvariationen höherer Ordnung. Diplom Arbeit, Ruhr-Universität, Bochum, Germany.

Frakes, L.A., Francis, J.E., Syktus, J.I., 1992. Climate Modes of the Phanerozoic: The History of the Earth's Climate over the Past 600 Million Years. Cambridge Univ. Press, Cambridge.

Garrels, R.M., Perry, E.A., 1974. Cycling of carbon, sulfur and oxygen throughout geologic time. In: Goldberg, E.D. (Ed.), The Sea. Wiley-Interscience, New York, pp. 303–336.

Goddéris, Y., François, L.M., 1996. Balancing the Cenozoic carbon and alkalinity cycles: constraints from isotopic records. Geophys. Res. Lett. 23, 3743–3746.

Golks, C., 1995. Strontiumisotopentrends höherer Ordnung, globales Signal oder lokale Trends? Diplom Arbeit, Ruhr-Universität, Bochum, Germany.

Grahn, Y.G., Caputo, M.V., 1992. Early Silurian glaciation in Brazil. Paleogeogr., Paleoclimatol., Paleoecol. 99, 9–15.

Gregory, R.T., 1991. Oxygen isotope history of seawater revisited: composition of seawater. In: Taylor, H.P., Jr., O'Neil, J.R., Kaplan, I.R. (Eds.), Stable Isotope Geochemistry: a Tribute to Samuel Epstein. Geochem. Soc. Spec. Publ., Vol. 3, pp. 65–76.

Gregory, R.T., Taylor, H., 1981. An oxygen isotope profile in a section of Cretaceous oceanic crust, Samail Ophiolite, Oman: evidence for $\delta^{18}O$ buffering of the oceans by deep (5 km) seawater hydrothermal circulation at mid-ocean ridges. J. Geophys. Res. 86, 2737–2755.

Grossman, E.L., Zhang, C., Yancey, T.E., 1991. Stable-isotope stratigraphy of brachiopods from Pennsylvanian shales in Texas. Geol. Soc. Am. Bull. 103, 953–965.

Grossman, E.L., Mii, H.-S., Yancey, T.E., 1993. Stable isotopes in late Pennsylvanian brachiopods from the United States: implications for Carboniferous paleoceanography. Geol. Soc. Am. Bull. 105, 1284–1392.

Grossman, E.L., Mii, H.-S., Zhang, C., Yancey, T.E., 1996. Chemical variation in Pennsylvanian brachiopod shells — effects of diagenesis, taxonomy, microstructure and paleoenvironment. J. Sediment. Res. 66, 1011–1022.

Harland, W.B., Armstrong, R.L., Cox, A.V., Craig, L.E., Smith, A.G., Smith, D.G., 1990. A Geologic Time Scale. Cambridge Univ. Press, Cambridge.

Hayes, J.M., Strauss, H., Kaufman, A.J., this issue. The abundance of ^{13}C in marine organic matter and isotopic fractionation in the global biochemical cycle of carbon during the past 800 Ma. Chem. Geol.

Hess, J., Bender, M.L., Schilling, J.-G., 1986. Evolution of the ratio of Strontium-87 to Strontium-86 in seawater from Cretaceous to present. Science 231, 979–984.

Hess, J.L., Scott, D., Bender, M.L., Kennett, J.P., Schilling, J.-G., 1989. The Oligocene marine microfossil record: age assessments using strontium isotopes. Paleoceanography 41, 655–679.

Hodell, D.A., Woodruff, F., 1994. Variations in strontium isotopic ratio of the seawater during the Miocene: stratigraphic and geochemical implications. Paleoceanography 9, 405–426.

Hodell, D.A., Mueller, P.A., McKenzie, J.A., Mead, G.A., 1989. Strontium isotope stratigraphy and geochemistry of the late Neogene ocean. Earth Planet. Sci. Lett. 92, 165–178.

Hodell, D.A., Mead, G.A., Mueller, P.A., 1990. Variation in the strontium isotopic composition of seawater (8 Ma to recent): implications for chemical weathering states and dissolved fluxes to the oceans. Chem. Geol. 80, 291–307.

Hodell, D.A., Mueller, P.A., Garrido, J.R., 1991. Variations in the strontium isotopic composition of seawater during the Neogene. Geology 19, 24–27.

Hoefs, J., 1997. Stable Isotope Geochemistry. Springer-Verlag, Berlin.

Hudson, J.D., Anderson, T.F., 1989. Ocean temperatures and isotopic compositions through time. R. Soc. Edinburgh Trans. Earth Sci. 80, 183–192.

Jacobsen, S., Kaufman, A.J., this issue. The Sr, C and O evolution of Neoproterozoic seawater. Chem. Geol.

James, N.P., Choquette, P.W., 1990. Limestones — the meteoric diagenetic environment. In: McIlreath, I.A., Morrow, D.W. (Eds.), Diagenesis. Geosci. Can. Repr. Ser., Vol. 4, pp. 35–73.

James, N.P., Bone, Y., Kyser, T.K., 1997. Brachiopod $\delta^{18}O$ values do reflect ambient oceanography: Lacepede Shelf, southern Australia. Geology 25, 551–554.

Jasper, T., 1999. Strontium-, Kohlenstoff- und Sauerstoff-isotopische Entwicklung des Meerwassers: Perm. RNDr. Thesis, Ruhr-Universität, Bochum, Germany.

Jones, C.E., 1992. Strontium isotopes in Jurassic and Early Cretaceous seawater. PhD Thesis, University of Oxford, Oxford, England.

Jones, C.J., Jenkyns, H.C., Coe, A.L., Hesselbo, S., 1994a. Strontium isotopic variations in the Jurassic and Cretaceous seawater. Geochim. Cosmochim. Acta 58, 3061–3074.

Jones, C.E., Jenkyns, H.C., Hesselbo, S.P., 1994b. Strontium isotopes in the early Jurassic seawater. Geochim. Cosmochim. Acta 58, 1285–1305.

Jux, U., Steuber, T., 1992. C_{carb} and C_{org} — Isotopenverhältnisse in der silurischen Schichtenfolge Gotlands als Hinweis auf Meeresspiegelschwankungen und Krustenbewegungen. Palaontol. Monatsh. 7, 385–413.

Kampschulte, A., Strauss, H., 1996. The sulfur isotopic composition of Jurassic and Cretaceous seawater as deduced from trace sulfate in belemnites. J. Conf. Abstr. 1, 303.

Kampschulte, A., Strauss, H., 1998. The isotopic composition of trace sulphates in Paleozoic biogenic carbonates: implications for coeval seawater and geochemical cycles. Min. Mag. 62A, 744–745.

Karhu, J., Epstein, S., 1986. The implication of oxygen isotope records in coexisting cherts and phosphates. Geochim. Cosmochim. Acta 50, 1745–1756.

Kaufman, A.J., Knoll, A.H., Awramik, S.M., 1992. Biostratigraphic and chemostratigraphic correlation of Neoproterozoic sedimentary successions: upper Tindir Group, northwestern Canada, as a test case. Geology 20, 181–185.

Killingley, J.S., 1983. Effects of diagenetic recrystallization on $^{18}O/^{16}O$ values of deep-sea sediments. Nature 301, 594–597.

Knauth, L.P., Epstein, S., 1976. Hydrogen and oxygen isotope ratios in nodular and bedded cherts. Geochim. Cosmochim. Acta 40, 1095–1108.

Knoll, A.H., Hayes, J.M., Kaufman, A.J., Swett, K., Lambert, L.B., 1986. Secular variation in carbon isotope ratios from upper Proterozoic successions of Svalbard and east Greenland. Nature 321, 832–838.

Koepnick, R.B., Burke, W.H., Denison, R.E., Heatherington, E.A., Nelson, H.F., Otto, J.B., Waite, L.E., 1985. Construction of the seawater $^{87}Sr/^{86}Sr$ curve for the Cenozoic and Cretaceous: supporting data. Chem. Geol. Isot. Geosci. Sect. 58, 55–81.

Kolodny, Y., Epstein, S., 1976. Stable isotope geochemistry of deep sea cherts. Geochim. Cosmochim. Acta 40, 1195–1209.

Korte, C., 1999. $^{87}Sr/^{86}Sr$, $\delta^{18}O$, und $\delta^{13}C$ — Evolution des triassischen Meerwassers: Geochemische und Stratigraphische Untersuchungen an Conodonten und Brachiopoden. RNDr. Thesis, Ruhr Universität, Bochum, Germany.

Korvin, G., 1992. Fractals in flatland: a romance of <2 dimensions. In: Korvin, G. (Ed.), Fractal Models in the Earth Sciences. Elsevier, Amsterdam, pp. 87–118.

Kroopnick, P.M., 1985. The distribution of ^{13}C of CO_2 in the world oceans. Deep Sea Research 3, 57–84.

Kump, L.R., Arthur, M.A., this issue. Interpreting carbon isotope excursions: carbonates and organic matter. Chem. Geol.

Kürschner, W., Becker, R.T., Buhl, D., Veizer, J., 1993. Strontium isotopes in conodonts: Devonian–Carboniferous transition, the northern Rhenish Slate Mountains, Germany. Ann. Soc. Geol. Belg. 115, 595–622.

Land, L.S., 1995. Comment on 'Oxygen and carbon isotopic composition of Ordovician brachiopods: implications for coeval seawater' by H. Qing and J. Veizer. Geochim. Cosmochim. Acta 59, 2843–2844.

Lavoie, D., 1993. Early Devonian marine isotopic signatures: brachiopods from the upper Gaspé limestones, Gaspé Peninsula, Quebec, Canada. J. Sediment. Petrol. 63, 620–627.

Lecuyer, C., Reynard, B., 1996. High temperature alteration of oceanic gabbros by seawater (Hess Deep; Ocean Drilling Program Leg 147): evidence from oxygen isotopes and elemental fluxes. J. Geophys. Res. 101, 15883–15897.

Lindh, T.B., 1983. Temporal variations in ^{13}C, ^{34}S and global sedimentation during the Phanerozoic. MSc Thesis, University of Miami, Miami, FL, USA.

Lowenstam, H.A., 1961. Mineralogy, O-18/O-16 ratios, and strontium and magnesium contents of recent and fossil brachiopods and their bearing on the history of oceans. J. Geol. 69, 241–260.

Marshall, J.D., Brenchley, P.J., Mason, P., Wolff, G.A., Astini, R.A., Hints, L., Meidla, T., 1997. Global carbon isotopic events associated with mass extinction and glaciation in the late Ordovician. Paleogeogr., Paleoclimatol., Paleoecol. 132, 195–210.

Martin, E.E., McDougall, J.D., 1991. Seawater Sr isotopes at the Cretaceous/Tertiary boundary. Earth Planet. Sci. Lett. 104, 166–180.

Martin, E.E., McDougall, J.D., 1995. Sr and Nd isotopes at the Permian/Triassic boundary: a record of climate change. Chem. Geol. 125, 73–99.

McArthur, J.M., 1994. Recent trends in strontium isotope stratigraphy. Terra Nova 6, 331–358.

McArthur, J.M., Kennedy, W.J., Chen, M., Thirlwall, M.F., Gale, A.S., 1994. Strontium isotope stratigraphy for Late Cretaceous time: direct numerical calibration of the Sr isotope curve based on the US Western Interior. Paleogeogr., Paleoclimatol., Paleoecol. 108, 95–119.

McConnaughey, T.A., Whelan, J., 1997. Calcification generates protons for nutrient and bicarbonate uptake. Earth Sci. Rev. 42, 95–117.

McKenzie, J.A., Hodell, D.A., Mueller, P.A., Mueller, D.W., 1988. Application of strontium isotopes to late Miocene–early Pliocene stratigraphy. Geology 16, 1022–1025.

McKenzie, J.A., Isern, A., Elderfield, H., Williams, A., Swart, P.K., 1993. Strontium isotope dating of paleoceanographic, lithologic, and dolomitization events on the northeastern Australian margin, Leg 133. Proc. ODP, Sci. Res. 133, 489–498.

Miall, A.D., 1994. Sequence stratigraphy and chronostratigraphy: problems of definition and precision in correlation and their implications for global eustasy. Geosci. Canada 21, 1–26.

Middleton, P.D., Marshall, J.D., Brenchley, P.J., 1991. Evidence for isotopic changes associated with Late Ordovician glaciation, from brachiopods and marine cements of central Sweden. In: Barnes, C.R., Williams, S.H. (Eds.), Advances in Ordovician Geology. Geol. Surv. Can. Pap., Vol. 90, No. 9, pp. 313–323.

Mii, H.S., 1996. Late Paleozoic environments: carbon and oxygen isotope records and elemental concentrations of brachiopod shells. PhD Thesis, Texas A and M University, College Station, USA.

Mii, H.S., Grossman, E.L., Yancey, T.E., 1997. Stable carbon and oxygen isotope shifts in Permian seas of west Spitsbergen — global change or diagenetic artefact. Geology 25, 227–230.

Miller, K.G., Fairbanks, R.G., Mountain, G.S., 1987. Tertiary oxygen isotope synthesis, sea level history, and continental margin erosion. Paleoceanography 2, 1–19.

Milliman, J.D., 1974. Marine Carbonates. Springer-Verlag, New York.

Morrison, J.O., Brand, U., 1986. Geochemistry of recent marine invertebrates. Geosci. Canada 13, 237–254.

Muehlenbachs, K., 1998. The oxygen isotopic composition of the oceans, sediments and the seafloor. Chem. Geol. 145, 263–273.

Muehlenbachs, K., Clayton, R.N., 1976. Oxygen isotope composition of the oceanic crust and its bearing on seawater. J. Geophys. Res. 81, 4365–4369.

Oslick, J.S., Miller, K.G., Feigenson, M.D., Wright, J.D., 1994. Oligocene–Miocene strontium isotopes: stratigraphic revisions and correlations to an inferred glacioeustatic record. Paleoceanography 9, 327–443.

Pawellek, F., 1991. C- und O-Isotopie und Spurenelemente an Brachiopodenschalen aus dem Mitteldevon der Eifel. Diplom Arbeit, Ruhr-Universität, Bochum, Germany.

Perry, E.C., Tan, F.C., 1972. Significance of oxygen and carbon isotope variations in early Precambrian cherts and carbonate rocks of southern Africa. Geol. Soc. Am. Bull. 83, 647–664.

Peterman, Z.E., Hedge, C.E., Tourtelot, H.A., 1970. Isotopic composition of strontium in seawater throughout Phanerozoic time. Geochim. Cosmochim. Acta 34, 105–120.

Podlaha, O.G., 1995. Modellrechnungen auf der Basis hochauflösender Isotopen-stratigraphie (Sr, C, O) des Jura und der Unteren Kreide (Bajoc-Apt). RNDr. Thesis, Ruhr-Universität, Bochum, Germany.

Podlaha, O.G., Mutterlose, J., Veizer, J., 1998. Preservation of $\delta^{18}O$ and $\delta^{13}C$ in belemnite rostra from the Jurassic/early Cretaceous successions. Am. J. Sci. 298, 324–347.

Podlaha, O.G., Chalimourda, A., Albeverio, S., this issue. Nonlinear system analysis of $^{87}Sr/^{86}Sr$ time series for Phanerozoic seawater. Chem. Geol.

Popp, B.N., Anderson, T.F., Sandberg, P.A., 1986a. Brachiopods as indicators of original isotopic compositions in some Paleozoic limestones. Geol. Soc. Am. Bull. 97, 1262–1269.

Popp, B., Anderson, T.F., Sandberg, P.A., 1986b. Textural, elemental and isotopic variations among constituents in middle Devonian limestones. J. Sediment. Petrol. 56, 715–727.

Popp, N.B., Podosek, F.A., Brannon, J.C., Anderson, T.F., Pier, J., 1986c. $^{87}Sr/^{86}Sr$ in Permo-Carboniferous seawater from the analyses of well-preserved brachiopod shells. Geochim. Cosmochim. Acta 50, 1321–1328.

Qing, H., Veizer, J., 1994. Oxygen and carbon isotope composition of Ordovician brachiopods: implications for coeval seawater. Geochim. Cosmochim. Acta 58, 1501–1509.

Qing, H., Barnes, C.R., Buhl, D., Veizer, J., 1998. The Sr isotopic composition of Ordovician and Silurian brachiopods and conodonts: relationships to geological events and implications for coeval seawater. Geochim. Cosmochim. Acta 62, 1721–1733.

Quinn, T.M., Taylor, F.W., Halliday, A.N., 1994. Strontium-isotopic dating of neritic carbonates at Bougainville Guyot (Site 831), New Hebrides island arc. Proc. ODP, Sci. Res. 134, 89–95.

Railsback, L.B., 1990. Influence of changing deep ocean circulation on the Phanerozoic oxygen isotopic record. Geochim. Cosmochim. Acta 54, 1501–1509.

Rao, C.P., 1996. Oxygen and carbon isotope composition of skeletons from temperate shelf carbonates, eastern Tasmania, Australia. Carbonates and Evaporites 11, 169–181.

Raymo, M.E., Ruddiman, W.F., 1992. Tectonic forcing of late Cenozoic climate. Nature 359, 117–122.

Reissner, B., 1990. Stratigraphische und fazielle Untersuchungen im Mittel- und Oberdevon des Aachener Raumes, Nordeifel, Rheinisches Schiefergebirge. RNDr. Thesis, RWTH, Aachen, Germany.

Richter, F.M., DePaolo, D.J., 1987. Numerical models of diagenesis: application to DSDP 590B and the Neogene Sr isotopic evolution of seawater. Earth Planet. Sci. Lett. 83, 27–38.

Ruppel, S.C., James, E.W., Barrick, J.E., Nowlan, G., Uyeno, T.T., 1996. High-resolution $^{87}Sr/^{86}Sr$ chemostratigraphy of the Silurian: implications for event correlation and strontium flux. Geology 24, 831–834.

Rush, P.F., Chafetz, H.S., 1990. Fabric-retentive, non-luminescent brachiopods as indicators of original $\delta^{13}C$ and $\delta^{18}O$ composition: a test. J. Sediment. Petrol. 60, 968–981.

Sadler, P.M., 1981. Sedimentation rates and the completeness of stratigraphic sections. J. Geol. 89, 569–584.

Samtleben, C., Munneke, A., Bickert, T., Pätzold, J., 1996. The Silurian of Gotland (Sweden): facies interpretation based on stable isotopes in brachiopod shells. Geologische Rundschau 85, 278–292.

Sandberg, C.A., Ziegler, W., Bultynck, P., 1989. New standard conodont-zones and early *Ancyrodella* phylogeny across middle–upper Devonian boundary. Cour. Forschungsinst. Geol. Senckenberg 100, 195–230.

Schidlowski, M., Eichman, R., Junge, C.E., 1975. Precambrian sedimentary carbonates: carbon and oxygen isotope geochemistry and implications for the terrestrial oxygen budget. Precambrian Res. 2, 1–69.

Schindel, D.E., 1982. Resolution analysis: a new approach to the gaps in the fossil record. Paleobiology 8, 340–353.

Scholle, P.A., Arthur, M.A., 1980. Carbon isotopic fluctuations in Cretaceous pelagic limestones: potential stratigraphic and petroleum exploration tool. Am. Assoc. Petrol. Geol. Bull. 64, 67–87.

Schrag, D.P., this issue. Effects of diagenesis on the isotopic record of late Paleogene tropical sea surface temperatures. Chem. Geol.

Scotese, C.R., MacKinnon, D.I., Marlatt, J.R., Reilly, W.J., Smith, A.G., Stanford, B.D., 1994. Continental Drift, edn. 6. The PALEOMAP Project.

Shackleton, N.J., 1985. Oceanic carbon isotope constraints on oxygen and carbon dioxide in the Cenozoic atmosphere. Geophys. Monogr. 32, 412–417.

Smalley, P.C., Higgins, A.C., Howarth, R.J., Nicholson, H., Jones, C.E., Swinburne, N.H.M., Bessa, J., 1994. Seawater Sr isotope variations through time: a procedure for constructing a reference curve to date and correlate marine sedimentary rocks. Geology 22, 431–434.

Strauss, H., 1997. The isotopic composition of sedimentary sulfur through time. Paleogeogr., Paleoclimatol., Paleoecol. 132, 97–118.

Strauss, H., this issue. Geological evolution from isotope proxy signals: sulfur. Chem. Geol.

Struve, W., 1982. The Eifelian within the Devonian frame, history, boundaries, definitions. Cour. Forschungsinst. Geol. Senckenberg 55, 88–102.

Taylor, A.G., Lasaga, A.C., this issue. The role of basalt weathering in the Sr isotope budget of the oceans. Chem. Geol.

Thirwall, M.F., 1991. Long-term reproducibility and multicollector Sr and Nd isotope ratio analysis. Chem. Geol. Isot. Geosci. Sect. 94, 85–104.

Tucker, M.E., Wright, V.P., 1990. Carbonate Sedimentology. Blackwell, Oxford.

Veizer, J., 1983. Chemical diagenesis of carbonates: theory and application of trace element technique. In: Arthur, M.A., Anderson, T.F., Kaplan, I.R., Veizer, J., Land, L.S. (Eds.), Stable Isotopes in Sedimentary Geology, Vol. 10,. Society of Economic Paleontologists and Mineralogists Short Course Notes, pp. III-1–III-100.

Veizer, J., 1988. The earth and its life: systems perspective. Origins of Life 18, 13–39.

Veizer, J., 1989. Strontium isotopes in seawater through time. Ann. Rev. Earth Planet. Sci. 17, 141–167.

Veizer, J., Compston, W., 1974. $^{87}Sr/^{86}Sr$ composition of seawater during the Phanerozoic. Geochim. Cosmochim. Acta 38, 1461–1484.

Veizer, J., Hoefs, J., 1976. The nature of O^{18}/O^{16} and C^{13}/C^{12} secular trends in sedimentary carbonate rocks. Geochim. Cosmochim. Acta 40, 1387–1395.

Veizer, J., Holser, W.T., Wilgus, C.K., 1980. Correlation of $^{13}C/^{12}C$ and $^{34}S/^{32}S$ secular variations. Geochim. Cosmochim. Acta 44, 579–587.

Veizer, J., Fritz, P., Jones, B., 1986. Geochemistry of brachiopods: oxygen and carbon isotopic records of Paleozoic oceans. Geochim. Cosmochim. Acta 50, 1679–1696.

Veizer, J., Buhl, D., Diener, A., Ebneth, S., Podlaha, O.G., Bruckschen, P., Jasper, T., Korte, C., Schaaf, M., Ala, D., Azmy, K., 1997a. Strontium isotope stratigraphy: potential resolution and event correlation. Paleogeogr., Paleoclimatol., Paleoecol. 132, 65–77.

Veizer, J., Bruckschen, P., Pawellek, F., Diener, A., Podlaha, O.G., Jasper, T., Korte, C., Carden, G.A.F., Strauss, H., Azmy, K., Ala, D., 1997b. Oxygen isotope evolution of Phanerozoic seawater. Paleogeogr., Paleoclimatol., Paleoecol. 132, 159–172.

Wadleigh, M.A., Veizer, J., 1992. $^{18}O/^{16}O$ and $^{13}C/^{12}C$ in lower Paleozoic brachiopods: implications for the isotopic composition of sea water. Geochim. Cosmochim. Acta 56, 431–443.

Weber, J.N., 1965. The $^{18}O/^{16}O$ ratio in ancient oceans. Geokhimija 6, 674–680.

Weddige, K., 1977. Die Conodonten der Eifel-Stufe im Typusgebiet und benachbarten Faziesgebieten. Senckenbergiana Lethaea 58, 271–419.

Weddige, K., 1988. Eifel conodonts. Cour. Forschungsinst. Geol. Senckenberg 102, 103–110.

Wenzel, B., 1994. Isotopie und Geochemie Silurischen Brachiopoden (Gotland/Schweden). Diplom Arbeit, University of Erlangen/Nürnberg, Erlangen, Germany.

Wenzel, B., 1997. Isotopenstratigraphie silurischer Abfolgen und deren paleozeano-graphische Interpretation. Erlanger Geologische Abhandlungen 129, 1–117.

Wenzel, B., Joachimski, M.M., 1996. Carbon and oxygen isotopic composition of Silurian brachiopods (Gotland/Sweden): paleoceanographic implications. Paleogeogr., Paleoclimatol., Paleoecol. 122, 143–166.

Whittaker, S.G., Kyser, T.K., 1993. Variations in the neodymium and strontium isotopic composition and REE content of molluscan shells from the Cretaceous Western Interior seaway. Geochim. Cosmochim. Acta 57, 4003–4014.

Ziegler, W., 1962. Taxonomie und phylogenie oberdevonischer Conodonten und ihre stratigraphische Bedeutung. Hessisches Landesamt Bodenforschung Abhandlungen 87, 7–77.

Ziegler, W., Sandberg, C.A., 1990. The late Devonian standard conodont zonation. Cour. Forschungsinst. Geol. Senckenberg 121, 1–115.